Retrospective Theses and Dissertations

1965

Electron diffraction study of NH3, ND3, isobutyraldehyde, an N2O3-HF complex, and several cyclopropane derivatives

Jack Paul Guillory
Iowa State University

Follow this and additional works at: https://lib.dr.iastate.edu/rtd

Part of the Physical Chemistry Commons

ELECTRON DIFFRACTION STUDY OF NH_3, ND_3, ISOBUTYRALDEHYDE, AN

N_2O_3-HF COMPLEX, AND SEVERAL CYCLOPROPANE DERIVATIVES

by

Jack Paul Guillory

A Dissertation Submitted to the

Graduate Faculty in Partial Fulfillment of

The Requirements for the Degree of

DOCTOR OF PHILOSOPHY

Major Subject: Physical Chemistry

Approved:

In Charge of Major Work

Head of Major Department

Dean of Graduate College

Iowa State University
Of Science and Technology
Ames, Iowa

1965

TABLE OF CONTENTS

I. INTRODUCTION

A. Purpose

The present electron diffraction problem can be divided into three parts: (a) an investigation of the structures of NH_3 and ND_3, (b) a study of the conformational behavior of cyclopropyl carboxaldehyde, cyclopropyl methyl ketone, cyclopropane carboxylic acid chloride and isobutyraldehyde, and (c) an analysis of a complex of N_2O_3 and HF. Improved rotating sector techniques and refined microphotometry (1, 2, 3, 4) have made possible the attainment of diffraction data for these molecules of high accuracy.

The structural parameters of ammonia and deuteroammonia were determined for comparison with the corresponding spectroscopic values. It was hoped that isotope effects on the mean bond lengths and amplitudes of vibration could be observed for this system. An isotope effect on the bond lengths and mean amplitudes of CH_4 and CD_4 has been measured by Bartell et al. (5) using electron diffraction.

A new procedure for analysis was tested with the NH_3 and ND_3 diffraction data. Unsmoothed experimental intensities were compared with calculated intensities using a least squares technique (6). Analyses were also performed using the conventional radial distribution method in which manually smoothed total intensity curves are treated by Fourier techniques (7).

A series of carbonyl compounds with the formula RCOX was selected for analysis in order to investigate how changes in the R and X substituents affect internal rotation about the R-C single bond. Cyclopropyl

carbonyl compounds were studied in which the X group was a hydrogen atom, a methyl group and a chlorine atom, respectively. A study of the struc-ture of cyclopropyl carboxaldehyde itself is of interest because of the possibility suggested by physical organic chemists that it might simulate a nonclassical carbonium ion in some structural characteristics.

Isopropyl carboxaldehyde (i.e., isobutyraldehyde) was studied as a reference for comparison with cyclopropyl carboxaldehyde. The environ-ments of the R-C single bonds in these compounds are similar except for the carbon-carbon-carbon angle in the R group which is approximately 112° in the former and 60° in the latter. It was hoped that information on the form and barrier heights of the potentials which hinder rotation of the aldehyde group about the carbon-carbon bond in these two molecules could also be determined.

A $68^\circ C$ constant boiling complex was received from Dr. F. Seel who proposed that the vapor consisted of monomeric $NOF \cdot 6HF$ molecules (8). He also speculated that HF might trimerize to form two six-membered rings which could associate with an NOF molecule. As will be pointed out later, however, the existence of the $NOF \cdot 6HF$ compound is extremely unlikely, and the $68^\circ C$ boiling complex is actually an azeotrope of N_2O_3 and HF.

B. Previous Determinations

In 1940 Dennison (9) carried out a comprehensive analysis of the infrared spectrum of ammonia from which he determined its structural parameters. More recent infrared studies have been conducted by Palik (10) and Benedict and Plyler (11).

Structural parameters were also obtained by Weiss and Strandberg (12) from microwave measurements. A recent analysis of the Raman spectrum of ammonia was reported by Cummings and Welsh (13).

The mean bond lengths of NH_3 were determined from the electron diffraction investigation of Almenningen and Bastiansen (14). A more detailed electron diffraction study of both ammonia and deuteroammonia was carried out later by Bastiansen[1].

The structures and conformational behavior of cyclopropyl carboxaldehyde, cyclopropyl methyl ketone, cyclopropane carboxylic acid chloride and isopropyl carboxaldehyde have not been determined. A few analogous compounds have been investigated, however, as discussed below.

The cyclopropane molecule has been the subject of many theoretical and experimental studies. An electron diffraction investigation of its structure was conducted by Pauling and Brockway (15) in 1937. Subsequent studies were carried out by Bastiansen and Hassel (16), and Sinha (17). The most recent electron diffraction determination of the structure of cyclopropane was done by Bastiansen et al. (18).

The interatomic distances in the aldehydic portion of cyclopropyl carboxaldehyde should be similar to those in acetaldehyde. Structural studies of the latter molecule were performed by Ackermann and Mayer (19), Stevenson et al. (20), and Kilb et al. (21).

The molecular configuration of isopropyl carboxaldehyde has not been previously studied, but nuclear magnetic resonance and microwave studies

---

[1]Bastiansen, O., Chemical Institute, University of Oslo, Blindern-Oslo, Norway, Electron diffraction study of NH_3 and ND_3. Private communication. 1961.

have been conducted on the related molecule, propionaldehyde, by Abraham and Pople (22), and Butcher and Wilson (23), respectively. Although these temperature dependent methods have certain limitations, both investigations suggest that the gauche form is more stable than the s-trans with a Δ H difference of approximately 1.0 kcal/mole.

The molecular structure of NOF·6HF has not been established if, indeed, the molecule exists at all. The structures of its two components, NOF and HF, are known, however. Magnuson (24) has determined the bond lengths and angles in nitrosyl fluoride, whereas Naude and Verleger (25), and Bauer et al. (26) have studied the monomer and polymer forms of hydrogen flouride, respectively. The self-association of HF vapor has been investigated by Smith (27), Franck and Meyer (28), Briegleb and Strohmeier (29), and Maclean et al. (30).

As will be shown later, the alleged NOF·6HF complex was actually an azeotrope of N_2O_3 and HF. The structure of NO_2, one of the decomposition products of N_2O_3, has been studied by Moore (31) and Bird (32). The bond length in NO, the other decomposition product, has been determined by Bartell and Kuchitsu (33), and Nichols et al. (34).

II. EXPERIMENTAL PROCEDURE

A. Apparatus

The electron diffraction unit used in this investigation was con-
structed at Iowa State University. It is similar to the apparatus
constructed at the University of Michigan by Bartell and Brockway (1).

The electron beam is accelerated by a potential difference of 40,000
volts and focused on the photographic plates by a magnetic lens. Diffrac-
tion patterns are recorded on Kodak 4" x 5" process plates using an r^3
rotating sector of 48 millimeter radius. This heart-shaped sector
compensates for the steep drop-off in intensity of the scattered electrons
with increasing scattering angle.

The specimen injection system consists of a platinum nozzle, a
sample bulb and a stopcock-microswitch attachment. Whenever the stopcock
is opened, the microswitch triggers the electrostatic shutter so that
the electron beam and the emerging gaseous sample beam intersect for a
specified length of time. The sample pressure and exposure time are
carefully determined and controlled to reduce extraneous scattering.
Exposure times used in this study ranged from 2 to 45 seconds depending
on the sample being studied and the distance from the nozzle to the
photographic plate.

Diffraction data from the 21 and 11 centimeter camera distances
employed in this study cover the range from $s = 4.0$ $\overset{o}{A}^{-1}$ to $s = 40.0$ $\overset{o}{A}^{-1}$
where s is the scattering variable $(4\pi/\lambda)\sin(\phi/2)$, λ is the wavelength
of the electron beam and ϕ is the scattering angle. The camera lengths
are measured with a high precision cathetometer.

Intensities of diffraction patterns are determined by measuring the absorbancies of four apparently flawless plates for each camera distance. These measurements are made with a modified Sinclair Smith microphotometer in conjunction with a voltage-to-frequency converter and a Hewlett Packard electronic counter-digital recorder system. The instrument has a random fluctuation of less than one-tenth of one percent of the intensity measurements.

During microphotometry the plates are rotated at 600 rpm to average out possible defects in the photographic emulsion. Voltage readings are recorded at quarter-millimeter intervals starting at the outer edge of the plate and progressing across the center to the opposite edge. Since both the right and left hand sides of the spinning plates are read, eight measurements in all are averaged at each particular value of s.

The coupling of the refined rotating sector technique with precision microphotometry has made possible the attainment of high accuracy. This is accomplished only with an enormous increase in computational work which makes it necessary to use digital computers. For this analysis, IBM 650 and 7074 computers were utilized for converting voltage data into intensity values. Most of the calculations associated with the reduced molecular intensity function and the radial distribution function were also carried out using these computers.

B. Method of Analysis

1. Calculation of reduced intensity function

After the photographic plates are read with the microphotometer, the mean absorbancies, $\bar{A}$, are calculated from the measured voltages. In the

following equations, the subscript R refers to the measurements made from

the right outer edge of the plate to the center; the subscript L refers

to those measurements made from the center to the left outer edge.

$$\overline{A} = (A_R + A_L)/2 - (1/4.6) D \tag{1}$$

where $D = (\Delta V - \Delta V_0)/(V_M - V_0^f) + \Delta V_0/(V_R - V_0^i)$,

$A_R = \log [(V_{100} - V_0^i)/(V_R - V_0^i)]$,

$A_L = \log [(V_{100} - V_0^i)/(V_L - V_0^i)]$,

V_0^i and V_0^f are the initial and final voltages, respectively,

measured with the shutter closed,

V_{100} is the initial voltage at a clear portion of the plate measured

with the shutter open,

$\Delta V_0 = (V_0^i - V_0^f)$,

$\Delta V = (V_R - V_L)$ at $r = 43.75$ millimeters and

$V_M = V_R$ at $r = 43.75$ millimeters.

A plot of the difference between the two sets of absorbancies for

each plate indicates the centering error for that particular plate and

the amount of random scatter in the readings caused by microphotometer

fluctuations. A set of absorbancies is considered usable if the undula-

tions due to the centering error are no more than 0.4% and the fluctua-

tions due to random scatter are less than 0.1% of the absorbancies. The

absorbancy difference, ΔA, is calculated using

$$\Delta A = (A_R - A_L) + (1/2.3) D [(r - r_{min})/(r_{max} - r_{min})] \qquad (2)$$

where r is the plate radius. The terms in Equations 1 and 2 which contain the quantity D are the corrections for the voltage drift of the microphotometer-converter system.

The next step in the analysis is to convert absorbancies to average intensities by

$$\bar{I} = \sum_{i}^{N} \bar{A}_i (1 - \alpha \bar{A}_i)/N \qquad (3)$$

where α is the photographic emulsion calibration constant (5), and N is the number of plates to be averaged.

Leveled total intensities are calculated from the expression

$$I_o(q) = (\bar{I}_i - I_e)(1 + (r/L)^2)^{3/2}(\phi_{sc}/r^3)/I_A \qquad (4)$$

where the quantity $(1 + (r/L)^2)^{3/2}$ corrects for inverse square fall off of the intensity on the flat photographic plate. The sector correction term is ϕ_{sc}/r^3 and the extraneous scattering correction is $I_e = [ar^2 + \alpha(ar^2)^2] E^{ext}$ where a, α and E^{ext} are constants. The theoretical atomic intensity, I_A, used to level the intensities is given by

$$I_A = \sum_{k} \left\{ [Z_k - F_k(q)]^2 + S_k(q) \right\} /q^4 \qquad (5)$$

where Z_k is the atomic number of the kth atom,

$F_k(q)$ is the elastic atomic scattering factor,

$S_k(q)$ is the inelastic atomic scattering factor and

q is the scattering variable $(40/\lambda)\sin(\phi/2)$.

The elastic scattering factors are computed from approximations of the

type (35, 36)

$$F_k(q) = \sum_n a_n/(1 + b_n q^2)^{1_n} \tag{6}$$

where a, b, and l are constants. The inelastic scattering factor is
approximated by the analytical expression (37)

$$S_k(q) = B_k[1 - 0.200/(1 + 4.252v^2) - 0.302/(1 + 9.907v^2)^2$$
$$- 0.217/(1 + 31.9v^2)^4 - 0.216/(1 + 108.2v^2)^8] \tag{7}$$

where B_k is a constant and $V = 0.176\pi q/(10z_k^{2/3})$.

A smooth background intensity curve, I_B, is drawn through the total
intensity curve (4, 7). This background deviates from the ideal form of
a horizontal straight line because of errors in theory, varying sensitiv-
ity of the photographic emulsion, inadequate extraneous scattering
corrections, and inaccuracies in the sector correction. An experimental
representation of a reduced molecular intensity function, M(s), is now
derived from the relation

$$M(s) = (I_o(s)/I_B) - 1 \tag{8}$$

where $s = (\pi/10)q$.

Ideally, the M(s) function is defined as

$$M(s) = I_M/I_A = (I_{tot}/I_A) - 1 \tag{9}$$

where $I_{tot} = I_M + I_A$ (38), and I_M is the molecular intensity. In practice,
since the function I_A is not a direct observable, it is necessary to
resort to a plausible estimate, I_B, which can be refined as the analysis

proceeds.

The theoretical reduced molecular intensity function, $M(s)_{th}$, may be calculated from

$$M(s)_{th} = \underset{ij}{\Sigma\Sigma}' \; C_{ij}\mu_{ij}(s)e^{-(1_m^2)_{ij}s^2/2}(\cos \Delta \, \eta_{ij})$$

$$\times \; (\sin s(r_g(1)_{ij} + \phi(s)_{ij}))/s(r_e)_{ij} \tag{10}$$

where $C_{ij} = Z_iZ_j/\underset{k}{\Sigma}(Z_k^2 + Z_k)$,

$\mu_{ij} = [Z_i - F_i(s)][Z_j - F_j(s)] \; \underset{k}{\Sigma} \; (Z_k^2 + Z_k)/$

$\qquad Z_iZ_j \; \underset{k}{\Sigma} \; [(Z_k - F_k(s))^2 + S_k(s)]$,

$(1_m)_{ij}$ is the root mean square amplitude of vibration of the ij^{th} atom pair (39),

$\cos (\Delta \, \eta_{ij})$ is the phase shift correction due to the failure of the Born approximation (40),

$r_g(1)_{ij}$ is the center of gravity of the ij^{th} peak in the $f(r)$ function,

$\phi(s)_{ij}$ is the frequency modulation term associated with the ij^{th} anharmonic oscillator (5) and

$(r_e)_{ij}$ is the equilibrium distance of the ij^{th} atom pair.

2. Structural parameters from radial distribution function

The radial distribution function (7) is given by

$$f(r) = \int_{s=0}^{s\simeq 4} sM_c(s)_{th} \; e^{-bs^2} (\sin sr)ds + \int_{s\simeq 4}^{s_{max}} sM_c(s) \; e^{-bs^2}$$

$$x \; (\sin sr)ds \tag{11}$$

where $\exp(-bs^2)$ is a combination weighting function and damping factor to compensate for lack of diffraction data to $s = \infty$. The function $M_c(s)$ is given by $M(s) + \triangle M(s)$ where $\triangle M(s)$ is a function to correct for the variation of μ_{ij} in Equation 10 caused by scattering from planetary electrons (41). A constant coefficient molecular intensity function, $M_c(s)_{th}$, is grafted onto the experimental $M_c(s)$ data in the inacessible small s range. Values of $M_c(s)_{th}$ are computed from Equation 10 with the function μ_{ij} replaced by unity.

A synthetic radial distribution function, $f(r)_{th}$, can be calculated from Equation 11 using a theoretical rather than an experimental reduced intensity curve, $M_c(s)$. As will be seen in the discussion of the structure determinations of the cyclopropane derivatives, this relation is useful for comparison with $f(r)_{exp}$.

Corrections were made to the experimental radial distribution function for integral termination errors (42). The asymmetry of $f(r)_{exp}$ peaks was partially removed by the addition of the quantity

$$C = -K \sum_j \left\{ c_j a_j l_j / [6(r_e)_j (2b + l_j^2)^{1/2}] \right\} [l_j(r - (r_e)_j)/$$

$$(2b + l_j^2)]^3 \exp[-(r - (r_e)_j)^2/(4b + 2l_j^2)] \tag{12}$$

where a, K and b are constants. This correction converts the anharmonic $f(r)$ function to a nearly harmonic, or Gaussian radial distribution function, $f_c(r)$. Such adjustments are important when extreme accuracy is sought.

The final step in a structure analysis requires a knowledge of the rough structure of the molecule being studied. With this information a synthetic radial distribution function, $f(r)_{syn}$, can be computed varying the structural parameters to obtain the closest match with $f(r)_{exp}$. This is accomplished by minimizing the sum of the squares of the differences between the experimental function and the synthetic one. The synthetic function (7) used in the least squares analysis is represented by the equation

$$f(r)_{syn} = K \sum_j \left\{ c_j / [r_j (2b + 1_j^2)^{1/2}] \right\} \exp[-(r - r_j)^2 / (4b - 21_j^2)] \quad (13)$$

where K, c_j and b are constants.

The electron diffraction bond length obtained from the least squares analysis of the corrected radial distribution function, $f_c(r)$, is $r_g(c)$. It corresponds to the center of gravity of the peaks in $f_c(r)$, whereas the parameter sought, $r_g(0)$, corresponds to the center of gravity of the probability distribution function, $P(r)$, where

$$M_c(s) = c \int_0^\infty P(r) (\sin sr) / sr \, dr \quad (14)$$

and c is a constant related to the scattering power of atoms[2].

---

[2]Equation 10 was derived from Equation 14 using a Morse oscillator potential function (39).

The equation relating $r_g(c)$ to $r_g(0)$ is

$$r_g(0) \simeq r_g(c) + 1_\alpha^2/r_e + [3a^2/2r_e - 5a/2r_e^2 + 2/r_e^3$$

$$+ a/(4b + 21_\alpha^2)]1_\alpha^4 + \text{(gas delocalization corrections)} \tag{15}$$

where b is the constant in the artificial damping factor, $\exp(-bs^2)$,

    a is the Morse asymmetry constant and

    1_α is the harmonic root mean square amplitude of vibration (39).

The gas delocalization corrections (43) were not made in these experiments since the pressure build-up in the main diffraction chamber was negligible during the time of plate exposure.

3. Structural parameters from experimental intensity function

Two aspects of the f(r) analysis technique described above should be pointed out: (a) a considerable amount of manual data processing is sometimes necessary, and (b) operator judgement and manipulation of data is unavoidable in certain key steps. Although the first feature is sometimes desirable[3], the second factor cannot be overlooked. Operator judgement is used in drawing the smooth background curve, $I_B(q)$, through the oscillations in $I_0(q)$. The use of an analytical function calculated by the computer in place of a manually drawn background curve would help to make the analysis more objective. It would also reduce the amount of data to be manually processed.

In this least squares procedure (6), the observed total intensities

---

[3]When the approximate structure of the molecule being studied is in doubt, frequent pauses for re-evaluation are recommended.

are compared to a calculated intensity function, $[I_0(s)]_{calc}$. The latter is given by

$$[I_0(s)]_{calc} = I_b(s) [RM(s)_{th} + 1] \qquad (16)$$

where R is the index of resolution, $M(s)_{exp}/M(s)_{th}$, $M(s)_{th}$ is the theoretical reduced intensity function, and $I_b(s)$ is an analytical background function of the form

$$I_b(s) = A \exp(-\alpha s) + \sum_{n=o}^{N} a_n s^n . \qquad (17)$$

The constant α is selected to give the proper bend in the background at small s values; the coefficients A and a_n are varied during the analysis.

An initial trial background is obtained by using a least squares method to fit a calculated background, $[I_b(s)]_{calc}$, with the analytical function of Equation 17. The background, $[I_b(s)]_{calc}$, is computed from Equation 16 assuming trial values for the molecular parameters in $M(s)_{th}$ and using experimental $I_0(s)$ values. This is the only important step in the least squares analysis where operator judgement is exercised.

Refinement of the initial trial background is achieved by minimizing the weighted function

$$\sum_i w_i \left\{ [I_0(s)]_{calc} - [I_0(s)]_{obs} \right\}_i^2 . \qquad (18)$$

Both the molecular parameters and the background coefficients are allowed to vary. The observed intensity values, $I_0(s)$, consist of raw, unsmoothed data, as opposed to the manually smoothed reduced intensities used in the f(r) technique.

The least squares intensity method was used primarily with the NH_3

and ND_3 data. The manually drawn backgrounds used in the f(r) analysis compared quite well with the output polynomial backgrounds. Polynomials of degree five to eight were used in the latter. The structural parameters were also in good agreement, within the limits of the estimated error, with those obtained from the f(r) analysis.

Although the least squares intensity program was used quite success-fully with NH_3 and ND_3, its application is of limited utility in the analysis of very complex structures. The procedure requires more accurate trial values of molecular parameters for convergence than does the radial distribution analysis. Experience has shown that this new scheme is no real substitute for the older procedure. In some ways, however, it is a more powerful tool for obtaining optimum molecular parameters, and it also partially eliminates operator bias in electron diffraction determinations.

4. Internal rotation

A rough estimate of the barrier hindering free rotation of the aldehyde groups in cyclopropyl carboxaldehyde and isopropyl carboxaldehyde was obtained in this electron diffraction investigation. Once the skeletal parameters of a molecule are determined, the effect of the internal rotation on the radial distribution curve can be studied.

Internuclear separations involved in internal rotation are weighted over all angles of rotation by the distribution function $P(\theta) = N \exp(-V(\theta)/RT)$ where N is a normalizing factor and $V(\theta)$ is the potential function for internal rotation (44). The contributions to the M(s) function or the radial distribution function are then computed. For

cyclopropyl carboxaldehyde, the potential function was considered, for sake of analysis, to be represented by the relation

$$V(\theta) = V_0(1-\cos 2\theta)/2 \tag{19}$$

where V_0 is the potential barrier and θ is the angle of rotation measured from the s-trans position. The function used in the isopropyl carboxaldehyde analysis was

$$V(\theta) = V_1(1 + \cos \theta)/2 + V_3(1 - \cos 3\theta)/2 \tag{20}$$

where θ is the angle of rotation measured from the s-trans position and $3V_1/4$ is the approximate energy difference between the s-trans and gauche forms. The barrier to free rotation is approximately $V_3 + (V_1/2)$. All the torsion-dependent distances were calculated at 30° intervals of internal rotation of the aldehyde group about the carbon-carbon axis.

The potential function parameters V_0 and V_3 were varied and the contributions to the reduced molecular intensity function from the atom pairs involved in internal rotation were calculated. Subsequently, the corresponding synthetic radial distribution functions were computed. Approximate values of the potential function parameters for the two compounds could then be determined by comparing $f(r)_{exp}$ with the various $f(r)_{syn}$ curves.

5. Treatment of errors

An important part of every experimental analysis is the estimation of errors. Detailed discussions of errors in electron diffraction have been presented by Bartell et al. (5), Bonham and Bartell (7), Bastiansen

et al. (45), and Morino et al. (46). A brief review of an error analysis method is given below.

Experimental uncertainties of the parameters measured by electron diffraction fall into three classifications (41). First, there are systematic errors which primarily affect the determination of the bond distances rather than the vibrational amplitudes. Sources of these errors are: (a) the measurement of the scattering angle and, (b) the setting adjustments and calibration of the electron diffraction unit.

A second class of uncertainties consists of systematic errors in the intensity measurements. These errors have little affect on the bond distance determinations, but they do influence the amplitudes of vibration since they alter the degree of damping of the $M(s)_{exp}$ function rather than the nodal positions. Possible sources of systematic errors lie in the uncertainty of establishing a proper emulsion calibration constant or a suitable extraneous scattering correction. Errors in the vibrational amplitudes were estimated by

$$\sigma_R(1) = 0.7\ 1\ [\sigma(R)/R] \qquad (21)$$

where R is the index of resolution, 1 is the amplitude of vibration, and $\sigma(R)$ is the standard deviation of R.

A third group contains systematic and random errors which affect both the internuclear distance parameters and the amplitudes of vibration. These uncertainties are associated with the determination of the intensity as a function of the scattering angle and show up as base line fluctuations in the $f(r)_{exp}$ function. Uncertainty in the sector shape is a systematic error which belongs to this group, whereas microphotometer

fluctuations and emulsion irregularities are sources of random error.
The standard deviation of the bond distance, $\sigma(r)$, and the standard
deviation of the vibrational amplitude, $\sigma(l)$, were calculated using

$$\sigma(r) = 1.94 \ \sigma(f) \ (2b + l^2)^{1/2}/f_m \tag{22}$$

and

$$\sigma(l) = 1.33 \ \sigma(f) \ (2b + l^2)/lf_m \ , \tag{23}$$

respectively (7). The quantity, $\sigma(f)$, is the standard deviation of the
least squares fit of the $f(r)_{exp}$ function, b is the artificial damping
constant, l is the amplitude of vibration, and f_m is the maximum height
of the $f(r)_{exp}$ peak associated with the distance r.

After the diffraction pictures of cyclopropyl carboxaldehyde,
cyclopropyl methyl ketone, and isopropyl carboxaldehyde were taken, it
was discovered that the sector mounting inside the race had been slipping.
Consequently, the magnetic disturbance correction associated with the
incompletely demagnetized ball bearing race was not constant as had been
assumed. An additional random error of approximately 1 part per thousand
of the bond distance was therefore included for these molecules.

For a favorable case, the approximate contributions of the various
elements affecting the error in the bond distances are listed in Table 1.
The correction factor for sector slippage is not included.

Table 1. Estimated uncertainties in bond lengths for favorable case, parts per thousand (angstrom units)

Source	
Electron wavelength	0.2
Camera length	0.3
Gas spread	0.0 - 0.2
Sector imperfections	0.6
Fit of overall f(r) curve	0.8
Estimated net	1.1

III. STRUCTURE ANALYSES

A. Ammonia and Deuteroammonia

Samples of NH_3 and ND_3 were purchased from the Matheson Company and Merck and Company, Limited, respectively. Both compounds were 99.9% pure and the isotopic purity of deuteroammonia was greater than 98%.

Electron diffraction pictures of both substances were taken by Dr. K. Kuchitsu. Initial sample pressures of approximately 40 torr were used for the long camera range exposures, and pressures of approximately 60 torr were used for the middle camera range. Plate exposure times varied from 11 to 15 seconds for the long distance and 30 to 50 seconds for the middle distance.

After the photographic plates were read with the microphotometer-converter system, mean absorbancies and experimental intensities were calculated using the methods previously described. These computations were performed using the IBM 650 computer. Intensity curves for the long and middle camera distances of NH_3 and ND_3 are shown in Figures 1 and 2, respectively. The calculated background curves, $I_b(q)$, and the difference plots, $[I_o(q)]_{obs} - [I_o(q)]_{calc}$, illustrated in these figures will be discussed later.

The intensity curves for the long and middle distances were over-lapped at $q = 50$ and the theoretical intensity function was joined to the experimental curve at $q = 19$. Radial distribution functions were then calculated and are shown in Figure 3. A damping factor of $\exp(-0.00180s^2)$ was used. Indices of resolution were unity, to within the limits of experimental error.

Figure 1. Long distance intensity curves for NH_3 and ND_3. The experimental backgrounds (solid curves), $I_B(q)$, were selected to minimize negative regions in the corresponding experimental radial distribution curves. Calculated backgrounds (dashed curves), $I_b(q)$, were selected by the computer. The lower curves are the differences between the experimental and calculated intensity curves, $[I_o(q)]_{obs} - [I_o(q)]_{calc}$

LONG CAMERA RANGE
— EXP. INTENSITY
– – CALC. BACKGROUND
$\Delta I(q) = $ EXP. – CALC.

NH_3

ND_3

$I(q)$

$\Delta I(q)$
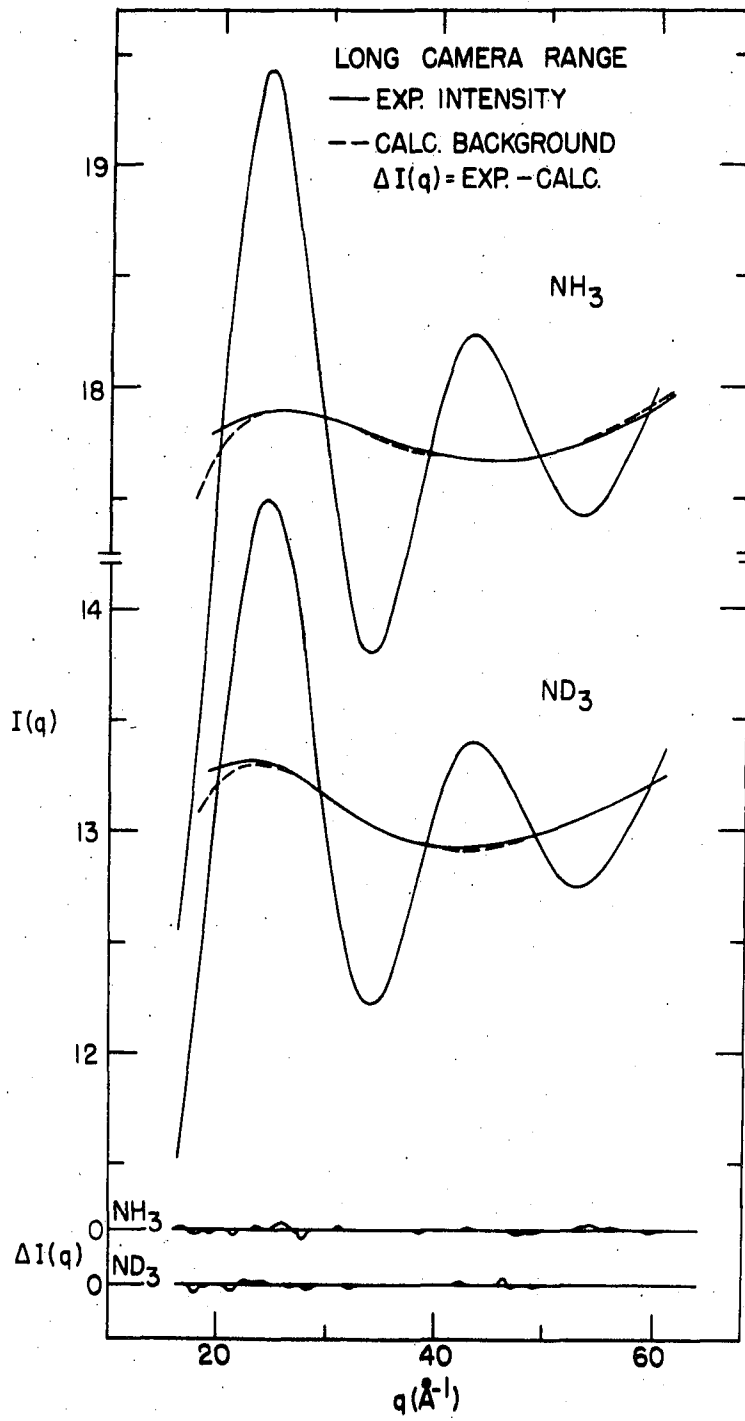
NH_3

ND_3

$q(\text{\AA}^{-1})$

Figure 2. Middle distance intensity curves for NH_3 and ND_3. The experimental backgrounds (solid curves), $I_B(q)$, were selected to minimize negative regions in the corresponding experimental radial distribution curves. Calculated backgrounds (dashed curves), $I_b(q)$, were selected by the computer. The lower curves are the differences between the experimental and calculated intensity curves, $[I_o(q)]_{obs} - [I_o(q)]_{calc}$

MIDDLE CAMERA RANGE
—— EXP. INTENSITY
—— CALC. BACKGROUND
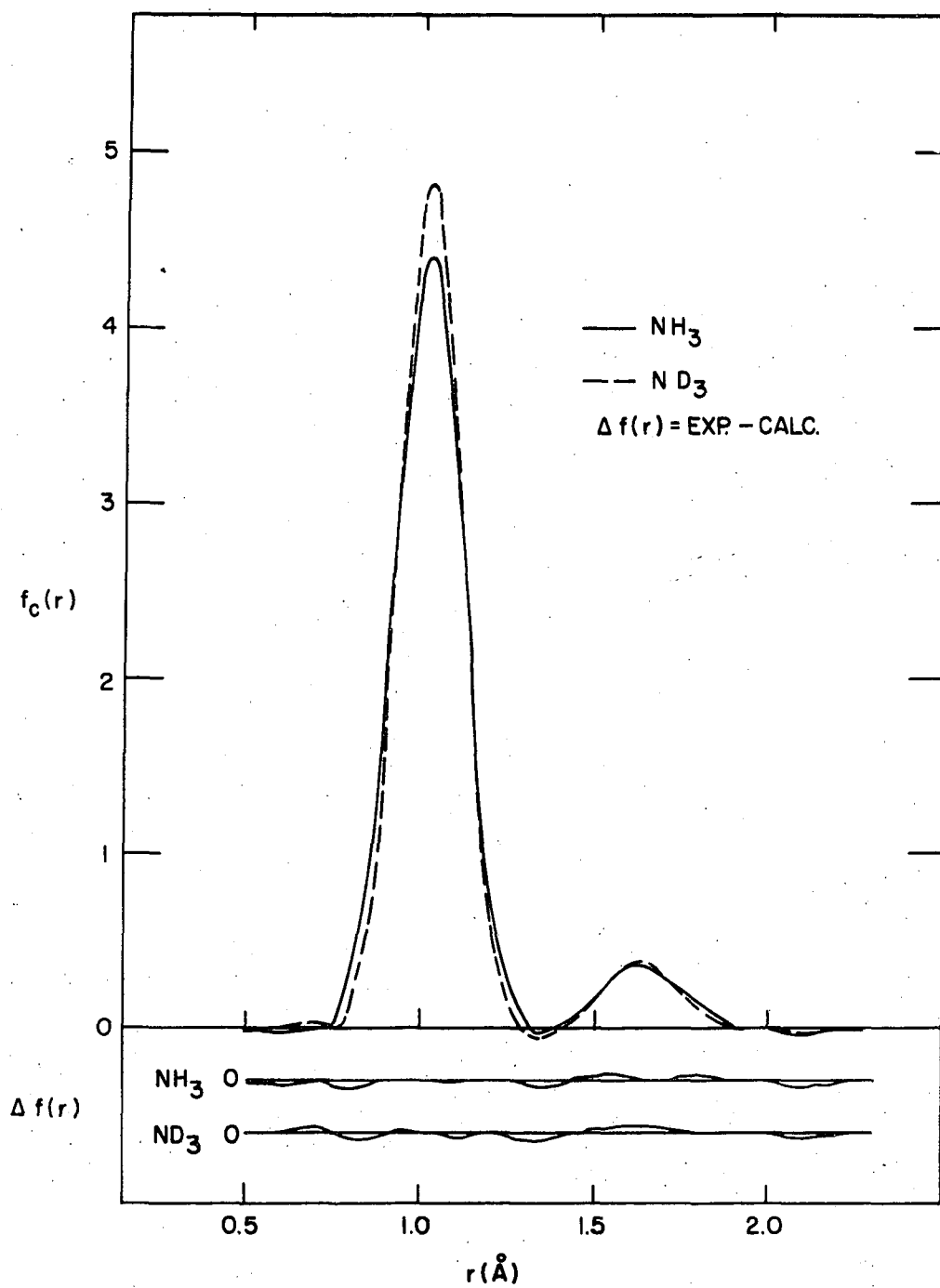
$\Delta I(q) = I(q)_{EXP} - I(q)_{CALC.}$
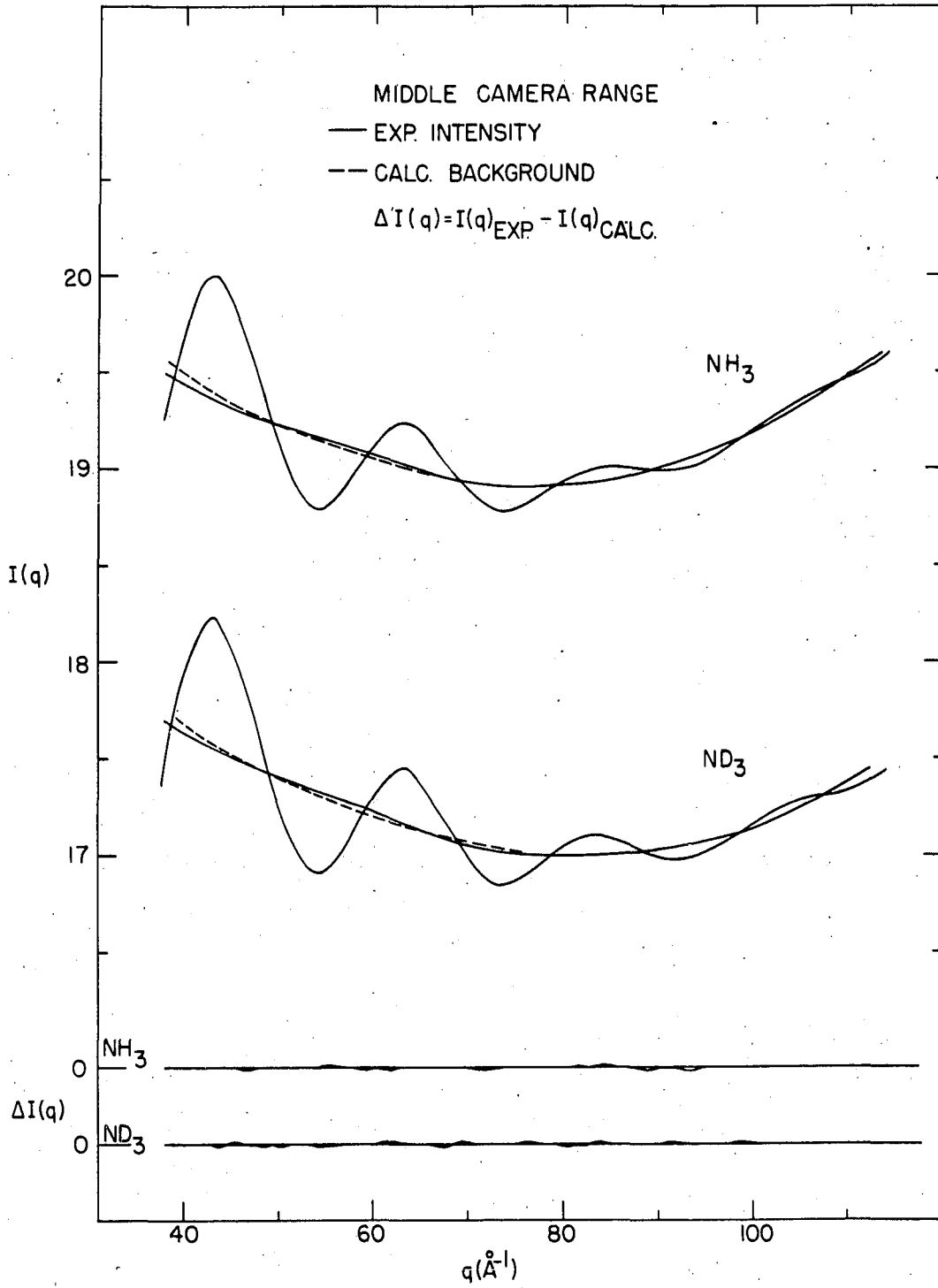
Figure 3. Corrected radial distribution curves for NH_3 and ND_3. Lower curves are the differences between experimental and calculated radial distribution functions

Results of the least squares analyses of the radial distribution functions are listed in Table 2. The mean bond length is greater for NH than for ND as a result of the larger amplitude of vibration of H atoms in the asymmetric force field of the molecule. In this determination, an isotope effect on the bond length of $[r_g(0)_{NH} - r_g(0)_{ND}] = 0.0025 \pm 0.0021$ Å was found. The effect is not unequivocally demonstrated, however, because of the large uncertainty. Smaller amplitudes of vibration in ND_3 also result in sharper ND and D··D peaks in the $f(r)$ curve, as can be seen in Figure 3.

Recent variational calculations of Ransil (47) indicate that the effective nuclear charge on hydrogen in hydride molecules is greater than the free atom value of unity. Bersohn (48) showed that the calculated field gradients for D-C≡ molecules were vastly improved by using $Z_{eff} = 1.2$ for the hydrogen atom in accounting for quadrupole moments. Bader and Jones (49) assigned an effective nuclear charge of 1.29 to the hydrogen 1s orbitals in the determination of the electron-density distribution for NH_3. Hence, the elastic scattering factor for the hydrogen atom was recalculated for an effective atomic number of 1.2 in order to test the sensitivity of the electron diffraction analysis to $(Z_H)_{eff}$. The new scattering factor was then used in computing the theoretical non-nuclear scattering, $\Delta M(s)$, for NH_3, and the radial distribution function was re-evaluated. A least squares analysis of the $f(r)$ curve indicated that using this effective atomic number produces a change in $r_g(NH)$ of less than 0.0002 Å and a change in $r_g(HH)$ of not more than 0.002 Å.

The raw intensity data of NH_3 and ND_3 were processed through the least squares intensity program previously described, using an IBM 7074

Table 2. Molecular parameters for ammonia and deuteroammonia derived from radial distribution analyses (in Å units)

Molecule	Distance	$r_g(0)$	$\sigma(r)$	l_g	$\sigma(l)$
NH_3	N-H	1.0289	0.0019	0.0734	0.0022
	H··H	1.644	0.014	0.090	0.012
	$\angle HNH = 106.03 \pm 1.32^o$				
ND_3	N-D	1.0264	0.0017	0.0623	0.0018
	D··D	1.645	0.011	0.077	0.010
	$\angle DND = 106.55 \pm 0.84^o$				

digital computer. Polynomial backgrounds of degree 4, 5, and 6 were used for the long distance intensities with $\alpha = 0.2$ in Equation 17. For the middle distance data, backgrounds of degree 7 and 8 were used neglecting the term $A \exp(-\alpha s)$ in Equation 17.

Calculated intensities and analytical background functions are shown in Figures 1 and 2. Standard deviations between calculated and experimental intensity curves were 6.8 and 6.2 parts per ten thousand for the long distance data of NH_3 and ND_3, respectively, with polynomial backgrounds of degree 5. Corresponding standard deviations for the middle distance data were 3.5 and 3.9 parts per ten thousand with backgrounds of degree 7. The use of the other polynomial backgrounds (i.e., those of degree 4 and 6) for the long distance data resulted in slightly larger standard deviations, but the output r_g and l_g parameters for the bonded distances differed by not more than 0.0013 Å from those obtained using backgrounds with 5 coefficients. Similar disagreements were observed

in comparing the 7 and 8 coefficient backgrounds of the middle distance

data for both NH_3 and ND_3. The corresponding differences for the non-

bonded parameters were less than 0.006 $\overset{o}{A}$ for the long distance data and

not more than 0.016 $\overset{o}{A}$ for the middle distance data.

Results of the least squares intensity analysis are reported in

Table 3. Indices of resolution for both camera distances of both mole-

cules were again essentially unity. The mean bond lengths and amplitudes

listed are weighted averages of the corresponding long and middle distance

values. The weighting factor used for each parameter was assumed to be

inversely proportional to the square of the standard deviation of that

parameter (50).

Bond lengths and amplitudes determined from the least squares

intensity analysis are in good agreement with those from the $f(r)$

analysis. Complete agreement was not expected, however, since the former

analysis used raw, unsmoothed intensity data while the $f(r)$ analysis used

manually smoothed data. Furthermore, the intensity analysis method does

not weight the data in the same way as the $f(r)$ analysis, and the system-

atic errors may influence the long and middle camera data differently.

The uncertainties computed from the intensity analysis (6) for the

nonbonded distances and amplitudes are small compared to those computed

from the $f(r)$ analysis. Experience has shown, however, that when

slightly different starting values of the trial nonbonded parameters are

used in the least squares intensity method, the output $H \cdot \cdot H$ and $D \cdot \cdot D$

parameters differ by 0.002 to 0.010 $\overset{o}{A}$ from those listed in Table 3. This

implies that the errors listed in the table should be larger. In view

of this lack of agreement between the $I_0(s)$ and $f(r)$ analyses, the larger

Table 3. Molecule parameters for ammonia and deuteroammonia derived from least squares intensity analyses (in $\overset{o}{A}$ units)

Molecule	Distance	$r_g(0)$	$\sigma(r)$	l_g	$\sigma(l)$
NH_3	N-H	1.0285	0.0011	0.0718	0.0015
	H··H	1.6607	0.0032	0.1116	0.0031
	$\angle HNH = 107.67 \pm 0.32°$				
ND_3	N-D	1.0259	0.0011	0.0577	0.0013
	D··D	1.6526	0.0018	0.0904	0.0022
	$\angle DND = 107.33 \pm 0.20°$				

error estimates in Table 2 seem more appropriate.

B. Cyclopropyl Carboxaldehyde

The properties of cyclopropyl derivatives have attracted increasing attention in recent years. These highly strained molecules have been the subject of many studies to determine the influence of molecular strain on bond lengths, bond angles, bond energies, and reactivities. The present investigation provides another striking manifestation of the distinction between bonds attached to cyclopropyl rings and bonds joined to unstrained saturated analogs.

A sample of cyclopropyl carboxaldehyde was donated by Professor C. H. DePuy. Gas phase chromatograms indicated that its purity was greater than 98%. The vapor from the liquid sample at room temperature was injected into the specimen chamber under its vapor pressure of approximately 38 torr. Exposure times of 2.3 and 6.9 seconds were used for the

long and middle distance plates, respectively. Four plates for the long

camera range and four for the middle distance were selected for micro-

photometering. Long and middle distance intensities were calculated and

the corresponding curves are found in Figure 4. Calculations involved

in the analysis of the data were done entirely on the IBM 7074 computer.

Several molecular configurations were considered in the structural

analysis. These include s-cis, s-trans and gauche isomers as illustrated

in Figure 5, and a configuration simulating that of a nonclassical

carbonium ion. In every synthetic radial distribution curve calculated

for mixtures of isomers with classical structures, it was assumed in

order to make the analyses tractable that: (a) all C-C bonds had the

same length, (b) all C-H bonds had the same length, (c) all ring C-C-H

angles were equal, and (d) bond lengths and angles did not depend on θ,

the angle of internal rotation. To the extent to which assumption (d)

is valid, the bonded and nearest nonbonded peaks of the 0 - 2.6 $\overset{o}{A}$ region

of the f(r) curve are independent of internal rotation. The principal

bond lengths and bond angles can therefore be determined without knowledge

of the distribution among rotational isomers.

The torsion-independent distances and root mean square amplitudes

of vibration were determined by a least squares resolution of the

experimental f(r) curve shown in Figure 6. Final results are listed in

Table 4. The errors for the C-H and C=O distances were calculated using

a method for estimating errors in composite peaks described by Bartell

and Carroll (51).

The relative strengths of the longest nonbonded peaks in the f(r)

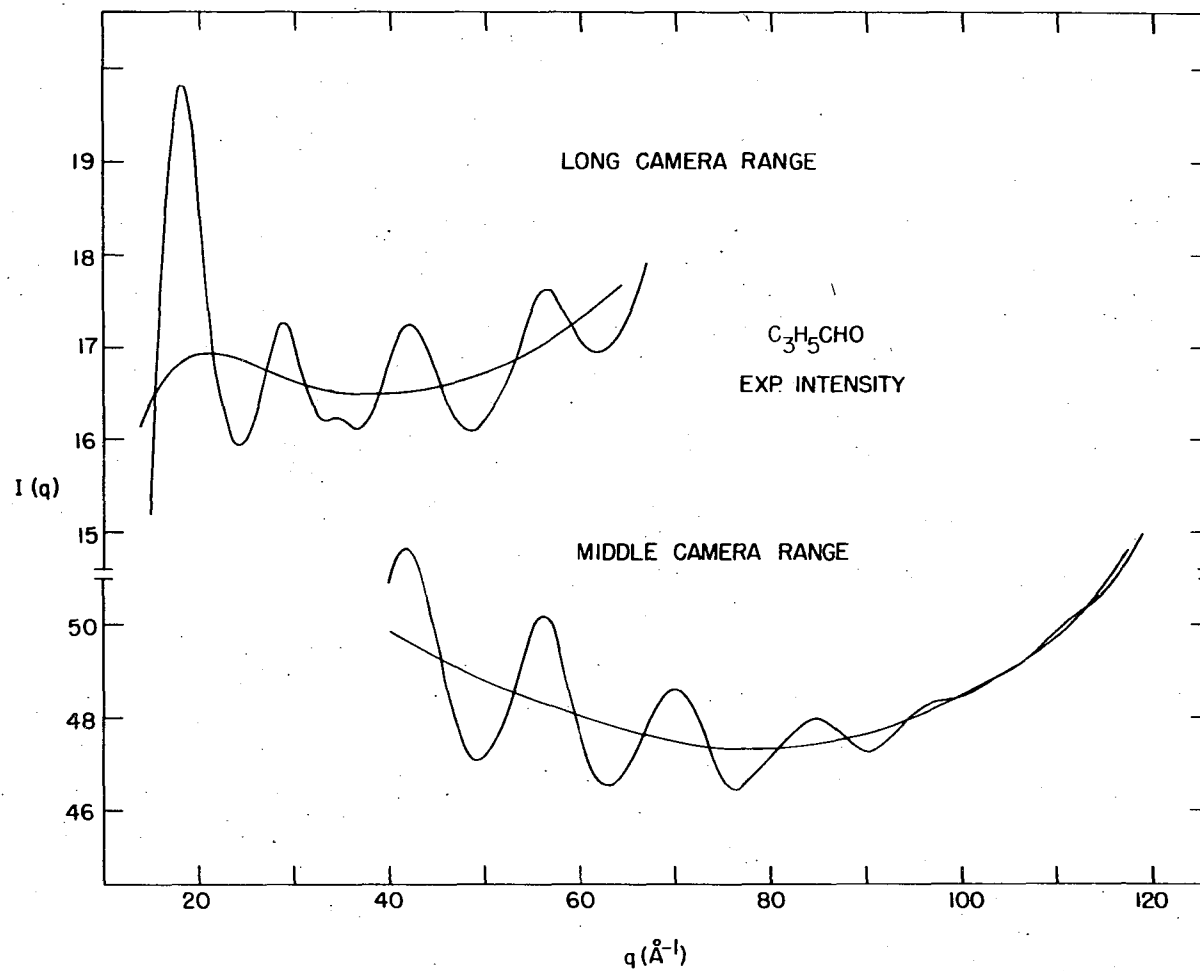curve are a measure of the distribution among the rotational isomers.

Figure 4. A plot of the experimental $I_o(q)$ and $I_B(q)$ functions for the long and middle camera distances of cyclopropyl carboxaldehyde
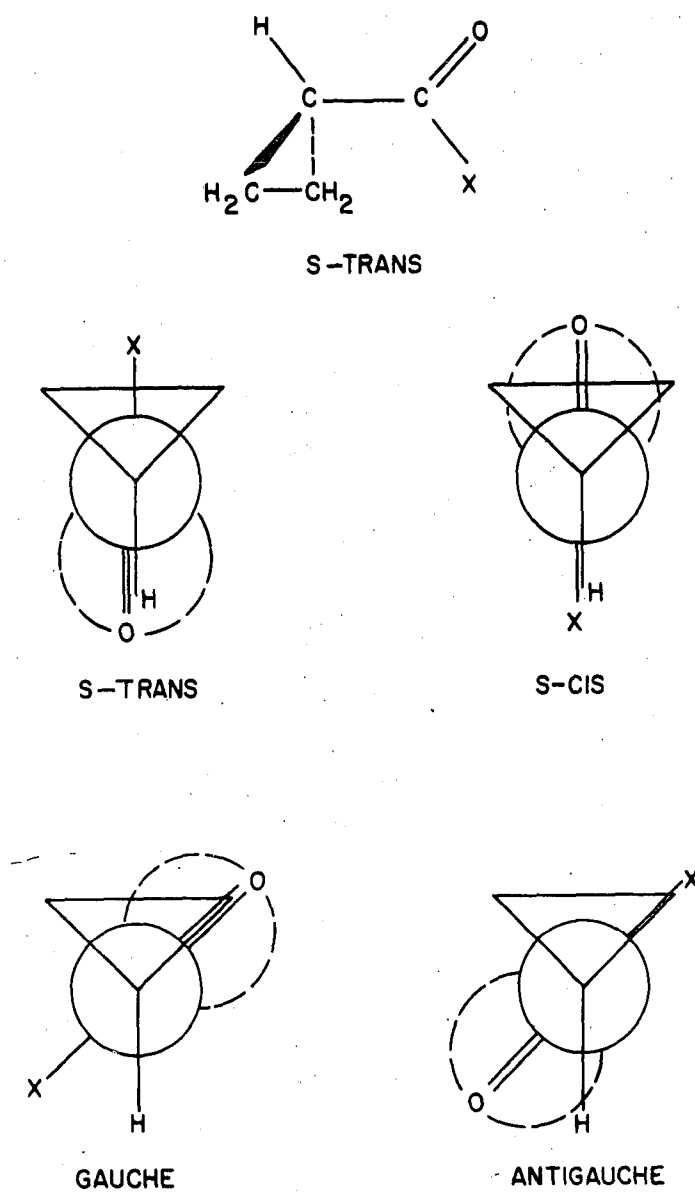
Figure 5. Conformational isomers of cyclopropane derivatives where the X group is a hydrogen atom, methyl group or chlorine atom
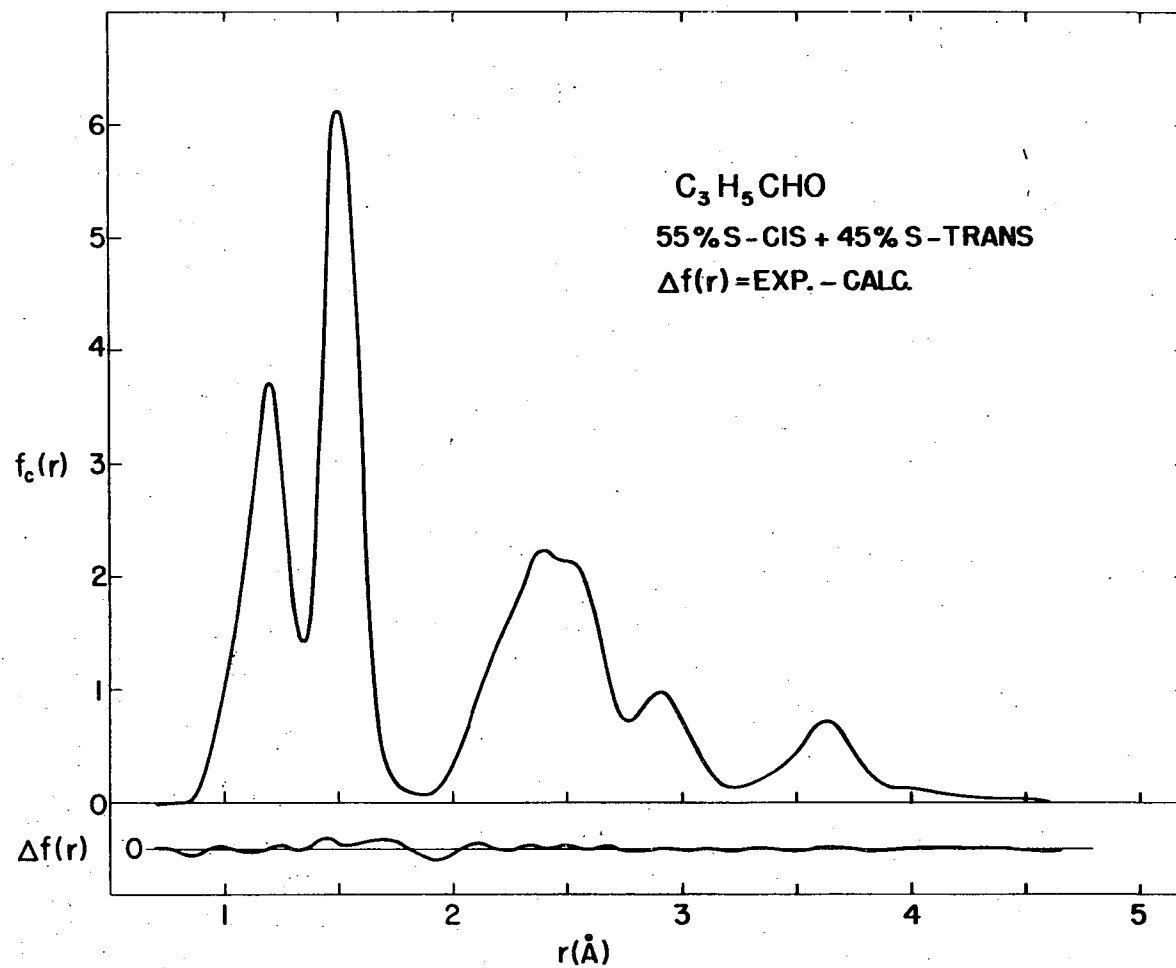
Figure 6. Corrected radial distribution curve for cyclopropyl carboxaldehyde with
an assumed rotational isomer distribution of 55% s-cis and 45% s-trans.
Lower curve is the difference between the experimental and calculated
radial distribution functions

Table 4. Molecular parameters for cyclopropyl carboxaldehyde derived
from radial distribution analysis (in Å units)

Distance	$r_g(0)$	$\sigma(r)$	l_g	$\sigma(l)$
C-H	1.115	+0.037,-0.021	0.087	+0.030,-0.004
C-C	1.507	0.002	0.056	0.002
C=O	1.216	+0.002,-0.018	0.046	+0.010,-0.006
C··O (cis)	2.925	0.009	0.103	0.007
C··O (trans)	3.641	0.007	0.093	0.006

$\angle CCO = 122.0 \pm 1.8°$, $\angle CCH_{aver} = 117.1 \pm 3.1°$

%s-cis = 55 ± 10, %s-trans = 45

For C_3H_5CHO, the most important distances are the 2.9 and 3.6 Å peaks
which can be ascribed to C··O distances in s-cis and s-trans conformers,
respectively. The absence of a peak in the 3.3 Å region indicates that
a gauche isomer cannot be present in appreciable concentrations.

Radial distribution curves were computed for several concentrations
of isomers, assuming reasonable values of skeletal parameters. Four dif-
ferent isomeric concentrations are illustrated in Figure 7. The curve
computed for a composition of 66.6% gauche and 33.3% s-trans isomers
represents the distribution corresponding to a simple 3-fold potential
barrier of the form found for acetaldehyde with minima at $\phi = \pm 60°$ and
$180°$.[4] The curve is clearly not acceptable. A second synthetic curve for

[4]The angle of rotation, θ, defined in Equations 19 and 20 is measured
from the s-trans position, whereas the "twist" angle, ϕ, is measured from
the s-cis position. As will become obvious later, certain isomers are
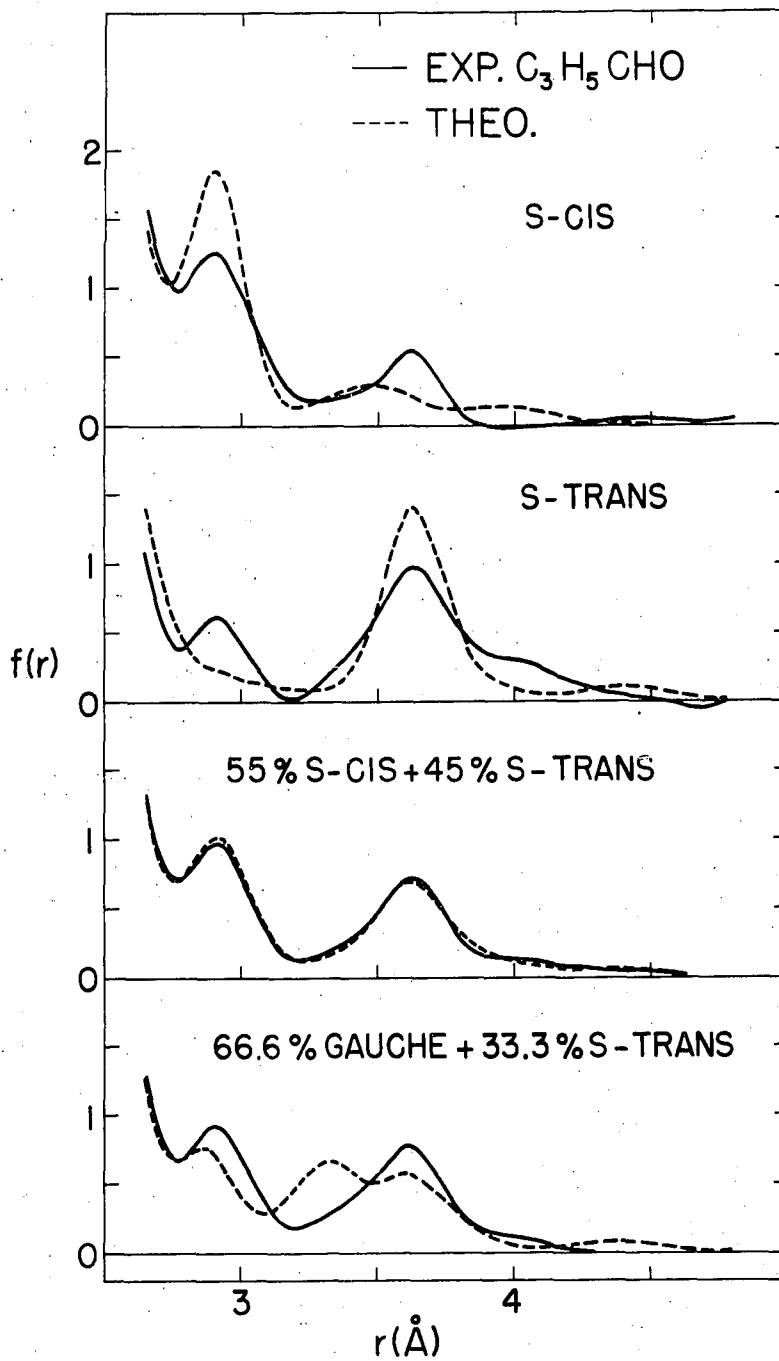more easily visualized in terms of the "twist" angle.

Figure 7. Experimental and calculated radial distribution curves for various isomeric concentrations of cyclopropyl carboxaldehyde

66.6% gauche and 33.3% s-trans calculated with the gauche angle narrowed

down to $\phi = \pm 33°$ was examined to test the possibility that ϕ(gauche) for

a cyclopropyl derivative might be smaller than for an acyclic derivative.

This curve is not within acceptable limits.

Least squares fittings of experimental f(r) curves by calculated

curves were run assuming various proportions of s-cis and s-trans isomers.

Distances and amplitudes were optimized for each assumed proportion. The

standard deviations between experimental and calculated curves in the range

from 2.6 to 4.7 $\overset{o}{A}$ imply that the equilibrium concentration is 55% s-cis

and 45% s-trans with an uncertainty of about $\pm$ 10%.

A structural model was considered in which the carbonyl carbon atom

was bent back over the cyclopropane ring to simulate the structure proposed

for a nonclassical carbonium ion. The best compromise to yield a corre-

spondence between experimental and calculated f(r) curves seemed to occur

for the following model. The CO bond was stretched to fall under the 1.50

$\overset{o}{A}$ peak and the C$\cdot\cdot$C and C$\cdot\cdot$O distances were adjusted to 2.56 and 2.90 $\overset{o}{A}$,

respectively. The comparison between calculated and observed f(r) curves,

as shown in Figure 8, lends no support for the existence of the nonclassi-

cal structure.

In the above analyses, rotational isomers were assumed to have fixed

values of θ. As previously discussed, the potential energy for internal

rotation of the carbonyl group in C_3H_5CHO was considered to have the form

$V_0(1-\cos 2\theta)/2$. Least squares fittings of the experimental f(r) curves

by calculated curves were run with various values of V_0 until optimum

structural parameters were obtained for each V_0. The standard deviations

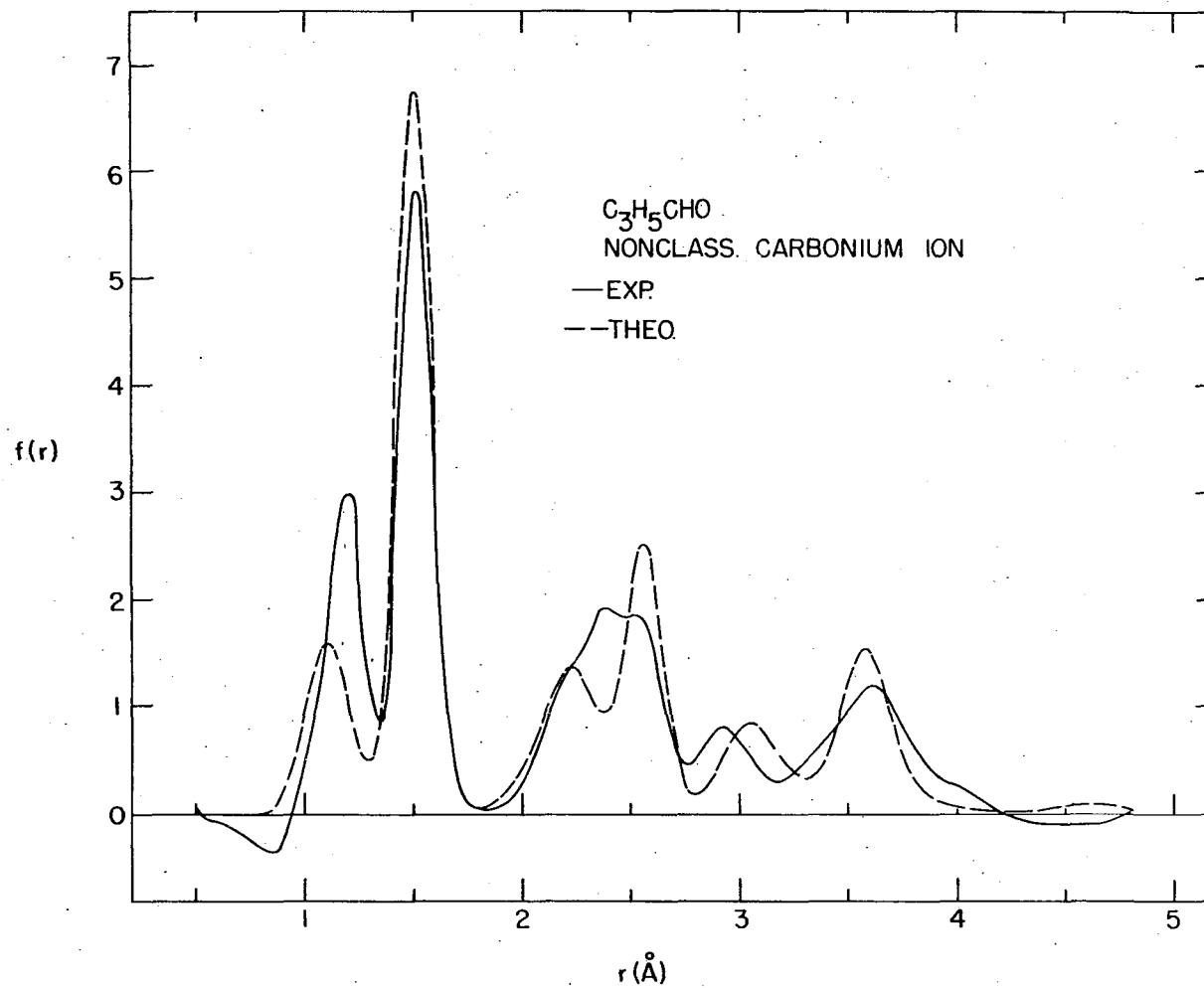between calculated and experimental curves suggest that the barrier is in

Figure 8. Experimental and calculated radial distribution curves for cyclopropyl carboxaldehyde using a nonclassical carbonium ion model

excess of 2.5 kcal/mole.

C. Cyclopropyl Methyl Ketone

A liquid sample of cyclopropyl methyl ketone was purchased from the Aldrich Chemical Company. Gas phase chromatograms of the fractionally distilled sample indicated that its purity was not less than 99%.

Diffraction patterns were taken at room temperature using a sample pressure of approximately 30 torr, the vapor pressure of $C_3H_5COCH_3$. Exposure times were 5.5 seconds for the long camera distance and 14 seconds for the middle camera distance. Experimental intensity curves used for calculation of the radial distribution functions are shown in Figure 9. Calculations were carried out on the IBM 7074 digital computer.

Various isomeric possibilities were considered in this analysis. In addition to the s-cis ($\phi = 0°$), s-trans ($\phi = 180°$) and gauche ($\phi = \pm 33°$ and $60°$) conformers (see Figure 5), an antigauche ($\phi = 147°$) configuration was tried in an effort to establish the distribution of isomers present. The reason for considering the latter isomer will be discussed later. As in the case of cyclopropyl carboxaldehyde, it was assumed that for all theoretical models tested the C-C bonds were the same length, all C-H bonds were the same length, and the ring C-C-H angles were all equal.

The experimental radial distribution curve is shown in Figure 10. The torsion-independent bond distances and amplitudes of vibration were determined from a least squares analysis of this curve. Final results are reported in Table 5.

At an early stage in this analysis it was realized that there was a
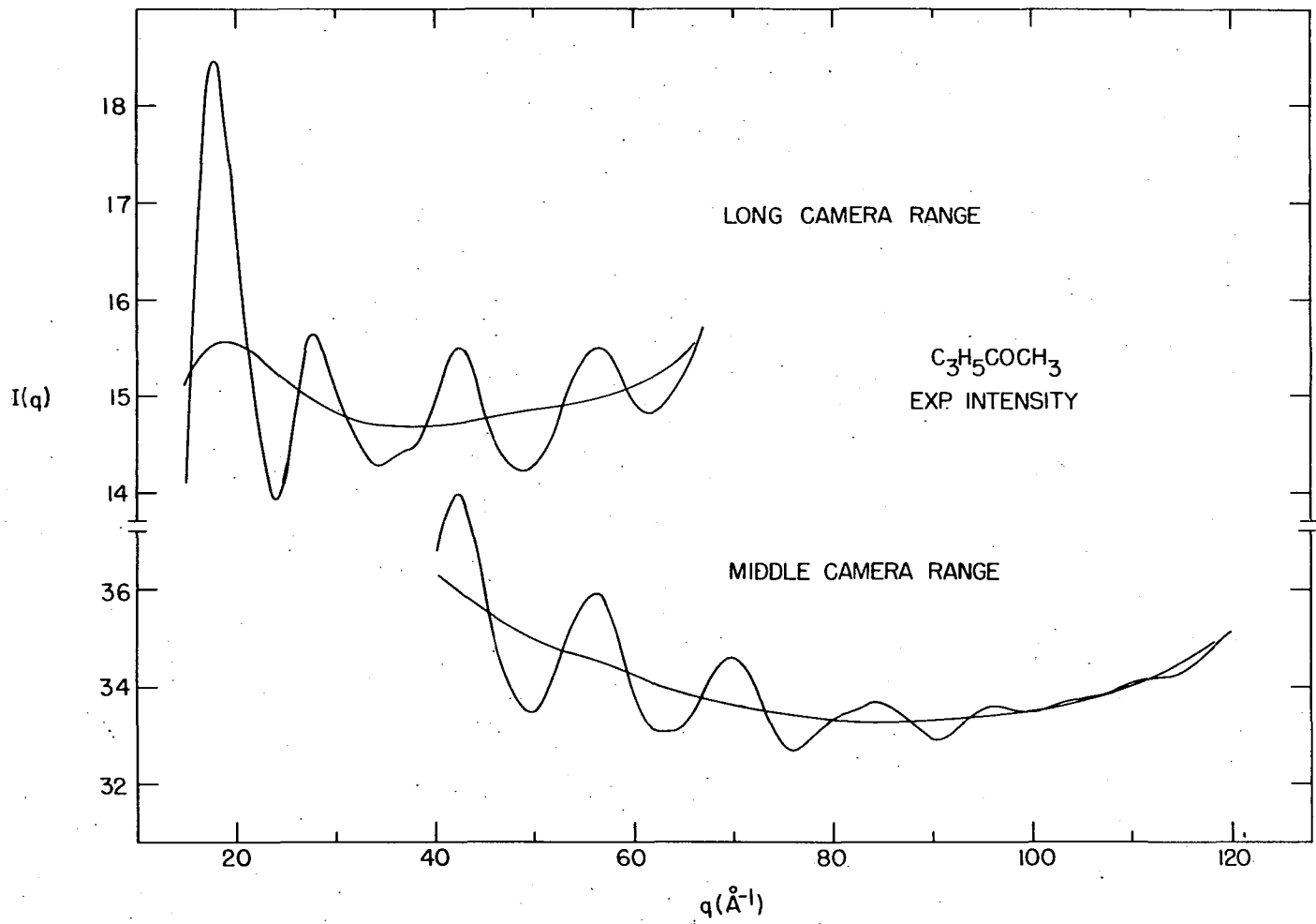
Figure 9. Experimental $I_o(q)$ and $I_B(q)$ functions for the long and middle camera distances of cyclopropyl methyl ketone

$C_3H_5COCH_3$

80% S-CIS + 20% ANTIGAUCHE
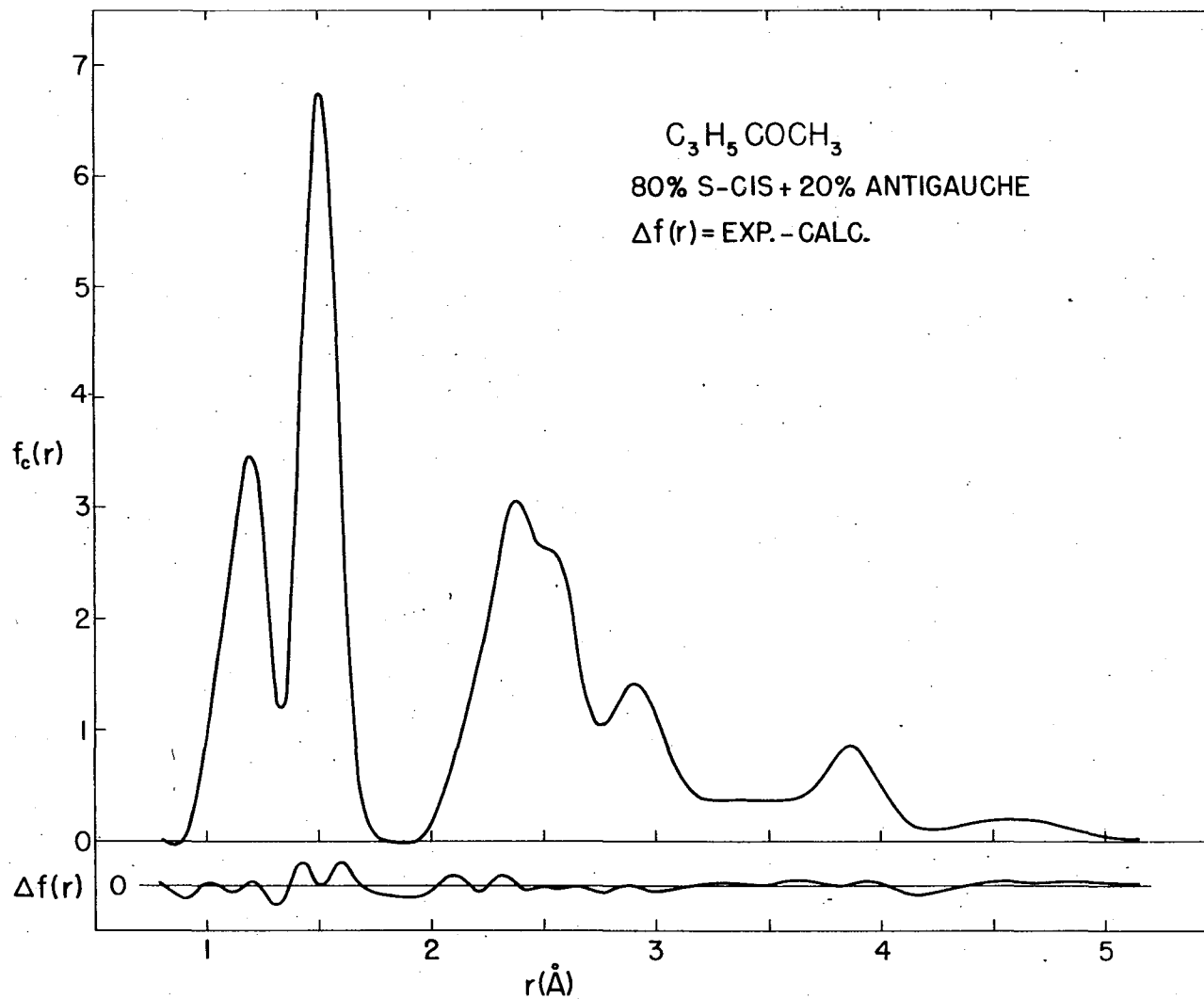
$\Delta f(r) = EXP. - CALC.$

Figure 10. Corrected radial distribution curve for cyclopropyl methyl ketone with an assumed rotational isomer distribution of 80% s-cis and 20% anti-gauche. Lower curve is the difference between the experimental and calculated f(r) curves

Table 5. Molecular parameters for cyclopropyl methyl ketone derived from radial distribution analysis (in $\overset{\circ}{A}$ units)

Distance	$r_g(0)$	$\sigma(r)$	l_g	$\sigma(l)$
C-H	1.126	0.015[a]	0.076	0.013[a]
C-C	1.510	0.003	0.048	0.003
C=O	1.225	0.011[a]	0.049	0.012[a]

$$\angle CCO_{aver} = 121.8 \pm 1.6^\circ, \quad \angle CCH_{aver} = 117.2 \pm 2.8^\circ$$

$$\%\underline{s}\text{-cis} = 80 \pm 15, \quad \% \text{ antigauche} = 20$$

[a]Because of severe overlapping of peaks in the f(r) curve from which these parameters have been obtained, the precision has been arbitrarily given by three times the standard deviation calculated using the independent peak formula.

substantial concentration of the $\underline{s}$-cis isomer. Preliminary $f(r)_{exp}$ curves exhibited peaks at 2.90 and 3.85 $\overset{\circ}{A}$ the positions and areas of which corresponded closely to those of a pure $\underline{s}$-cis model. These distances can be ascribed to the $O\cdot\cdot C_R$ and $C_M\cdot\cdot C_R$ distances in the latter where the subscript R refers to the ring atoms and M refers to the methyl group atoms. The absence of a peak in the 3.4 $\overset{\circ}{A}$ region indicates that essentially no gauche conformer is present. In this isomer, the longest $O\cdot\cdot C_R$ distance and the shortest $C_M\cdot\cdot C_R$ distance are approximately 3.4 $\overset{\circ}{A}$ in length.

Many different isomeric combinations were used in calculating radial distribution curves. Acceptable values of the skeletal parameters were assumed in all these cases. Five of the more informative concentrations are shown in Figure 11 for the 2.6 to 5.2 $\overset{\circ}{A}$ region of the f(r) curve. A comparison of the experimental and calculated curves for the pure $\underline{s}$-trans
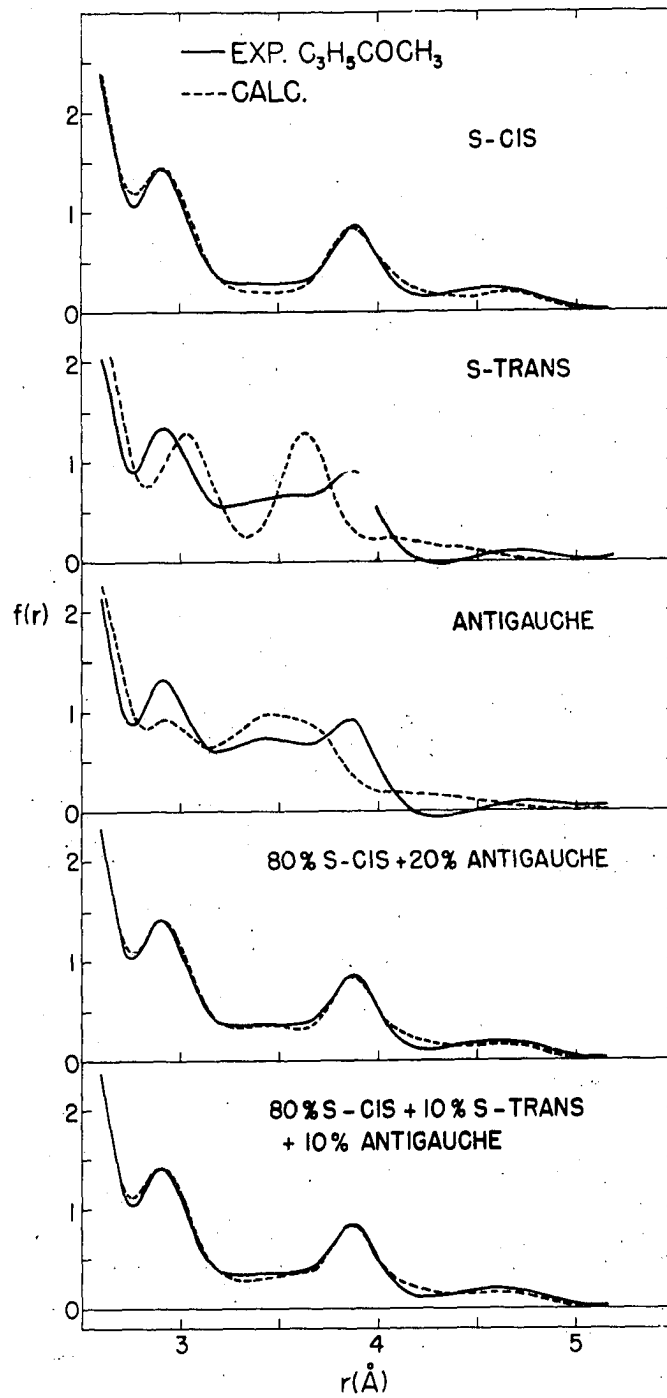
Figure 11. Experimental and calculated radial distribution curves for various isomeric concentrations of cyclopropyl methyl ketone

model indicates that this isomer cannot be present in large concentrations. This can be explained by noting that the closest $H_M \cdots H_R$ distance in the s-trans conformer is 2.02 $\overset{o}{A}$, whereas the sum of the corresponding van der Waals radii is 2.4 $\overset{o}{A}$ (52). Hydrogen-hydrogen repulsions, consequently, destabilize the s-trans isomer. They apparently stabilize an antigauche form ($\phi = 147^o$) where the methyl group eclipses the ring C-C bond and a distorted s-trans form where the C_M-C_O-C_R and C_O-C_R-H angles are distorted to increase the $H_M \cdots H_R$ distance to 2.30 $\overset{o}{A}$. The subscript 0 refers to the carbonyl carbon atom.

A least squares analysis of the experimental f(r) curves was carried out using calculated curves for various concentrations of s-cis, s-trans, distorted s-trans and antigauche isomers. The lowest standard deviation was obtained when the 80% s-cis + 20% antigauche model was used. An acceptable fit between experimental and calculated curves was also observed for the 80% s-cis, 10% distorted s-trans, and 10% antigauche theoretical model. The standard deviation associated with the f(r) curves computed for the concentration of 80% s-cis and 20% distorted s-trans isomers was at the outer limit of acceptability. This implies that the equilibrium concentration of $C_3H_5COCH_3$ consists of 80% s-cis isomer and 20% of a distribution of forms between the two antigauche positions (i.e., $\phi = 147^o$ to 213°) with an uncertainty of ± 15%.

D. Cyclopropane Carboxylic Acid Chloride

A sample of cyclopropane carboxylic acid chloride was purchased from the Aldrich Chemical Company and purified by fractional distillation. Its purity was checked with an Aerograph gas chromatograph and was estimated

to be not less than 98.5%.

The vapor from the liquid sample was injected into the diffraction chamber at room temperature and under a vapor pressure of approximately 14 torr. Plates were exposed for 2.7 seconds at the long camera range and 9.5 seconds at the middle camera range. The leveled intensity and background curves for the long and middle camera distances are shown in Figure 12.

Three configurations were originally considered in this analysis: (a) s-cis or "$0°$-twist" where $\phi = 0°$, (b) s-trans, and (c) gauche or "$33°$-twist". These configurations are pictured in Figure 5. The s-trans isomer tested is actually a distorted model where the $Cl-C_O-C_R$ and $C_O-C_R-C_R$ angles have been increased from $110°$ and $118°$ to $114°$ and $121.5°$, respectively, in order to increase the otherwise unduly short $Cl \cdot \cdot H_R$ nonbonded distance.

Those parameters which are independent of internal rotation were determined by a least squares resolution of the experimental $f(r)$ curve. The radial distribution function used in this analysis is shown in Figure 13. Final results are reported in Table 6.

Radial distribution curves were calculated for various assumed concentrations of isomers for comparison with the experimental curve in the 2.6 to 5.2 $\overset{o}{A}$ region. Five sets of these curves are shown in Figure 14. For C_3H_5COCl, the major nonbonded distances which depend upon internal rotation occur beyond 2.8 $\overset{o}{A}$ in the $f(r)$ curve. By comparing the experimental and theoretical curves computed for a pure s-trans configuration, it can be seen that a large concentration of this isomer does not exist.

Visual comparisons of the experimental and calculated $f(r)$ curves

Figure 12. Experimental $I_o(q)$ and $I_B(q)$ curves for the long and middle camera distances of cyclopropane carboxylic acid chloride

LONG CAMERA RANGE

C_3H_5COCl
EXP. INTENSITY

MIDDLE CAMERA RANGE

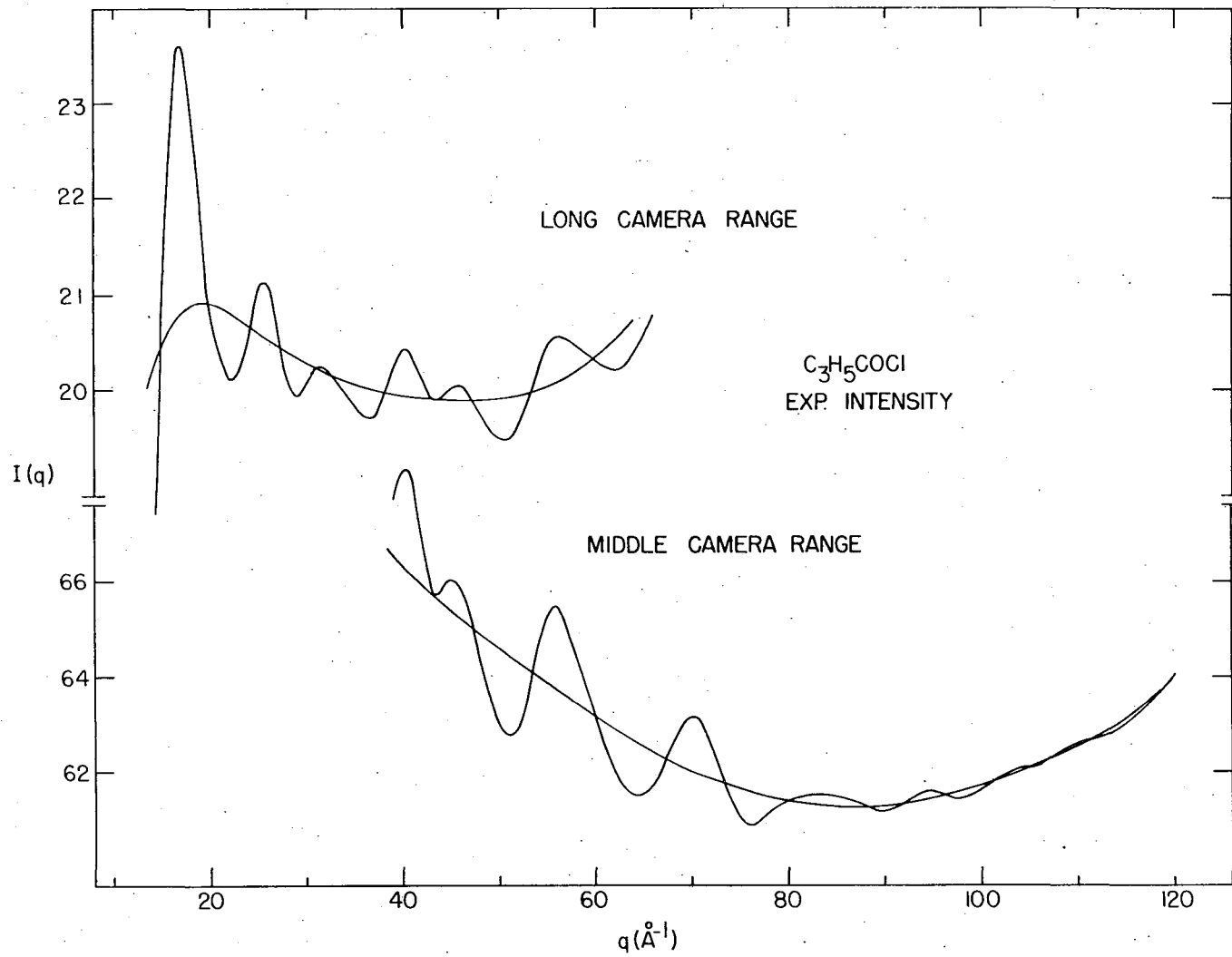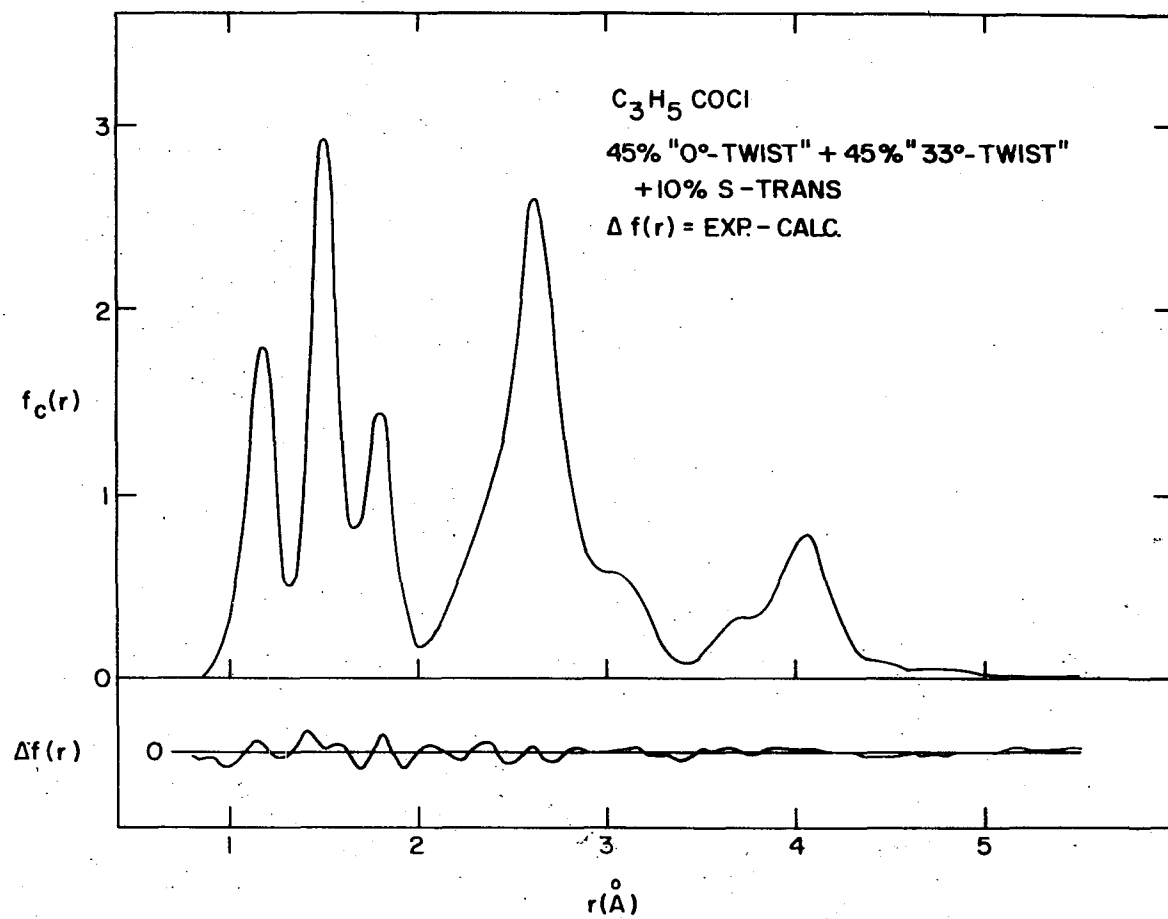I(q)

$q(\overset{\circ}{A}^{-1})$

46

Figure 13. A plot of the experimental radial distribution function for cyclopropane carboxylic acid chloride with an assumed distribution of 45% "0°-twist", 45% "33°-twist" and 10% s-trans isomers. The lower curve is a plot of the difference between the calculated and experimental radial distribution functions
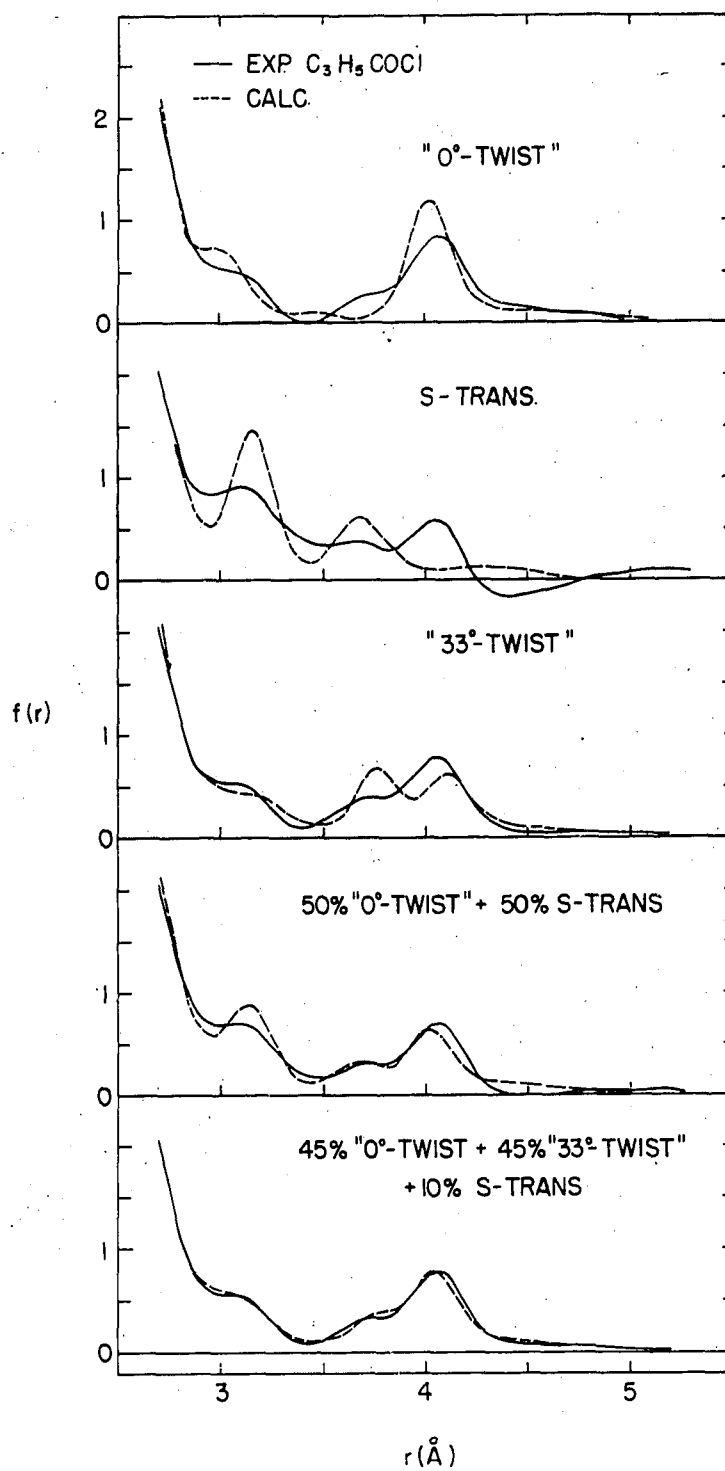
Figure 14. Experimental and calculated radial distribution curves for assumed isomeric concentrations of cyclopropane carboxylic acid chloride

Table 6. Molecular parameters for cyclopropane carboxylic acid chloride derived from the radial distribution function with an assumed distribution of 45% "0°-twist", 45% "33°-twist" and 10% s-trans isomers (in Å units)

Distance	$r_g(0)$	$\sigma(r)$	l_g	$\sigma(l)$
C-H	1.107	0.021[a]	0.082	0.018[a]
C-C[b]	1.506	0.002	0.049	0.002
C=O	1.197	0.009[a]	0.039	0.010[a]
C-Cl	1.797	0.009	0.071	0.009

$$\angle CCO^c = 127.6 \pm 2.9°, \quad \angle CCH^c_{aver} = 120.7 \pm 3.9°$$

$$\angle CCCl^c = 110.0 \pm 1.3°, \quad \angle OCCl^c = 122.4 \pm 1.4°$$

[a]Because of severe overlapping of peaks in the $f(r)$ curve from which these parameters were obtained, the uncertainties have been arbitrarily taken as three times the standard deviations calculated using the independent peak formula.

[b]All the C-C distances were assumed to be equal.

[c]These angles correspond to those in the "0°-twist" and "33°-twist" conformers, within the limits of experimental error.

suggested that the isomeric concentration in C_3H_5COCl is composed primarily of a continuous distribution of forms in the vicinity of the "0°-twist" conformer. In order to obtain a preliminary estimate of the equilibrium concentration, therefore, a least squares comparison was carried out using various proportions of only the s-trans, "0°-twist" and "33°-twist" isomers. Distances and amplitudes were optimized for each assumed proportion. The lowest standard deviation was obtained for a concentration of 50% "0°-twist", 40% "33°-twist" and 10% s-trans isomers.

A new least squares approach was also tested in this analysis. In

the first step, radial distribution curves for each isomer are computed.
The theoretical curves are then mixed to obtain the best fit with a
corresponding mixture of experimental $f(r)$ curves using a least squares
criterion. The molecular parameters themselves are not varied but are
kept geometrically consistent for each isomer model. For C_3H_5COCl, this
least squares mixing process yielded an equilibrium concentration of 42%
"$0°$-twist", 53% "$33°$-twist" and 5% s-trans conformers. A comparison of
the results of both least squares methods suggests that if the presumably
continuous distribution of isomers is represented, roughly, by "$0°$-twist",
"$33°$-twist", and s-trans components, the best fit is found for 45%,
45% and 10% concentrations, respectively.

In the "$0°$-twist" or s-cis configuration, the closest $Cl \cdot \cdot H_R$ distance
(where H_R is the tertiary hydrogen) is 2.7 $\overset{o}{A}$ as compared to the sum of
van der Waals radii of 3.0 $\overset{o}{A}$ (52). The resulting nonbonded repulsion
tends to destabilize the "$0°$-twist" form. In order to obtain more infor-
mation about the "twist" distribution, the $f(r)$ data were reprocessed
through the least squares mixing routine using $0°$, $15°$, $33°$ and $60°$ "twist"
theoretical models to represent, roughly, the continuous distribution in
∅ of the isomers. The best fit was obtained with concentrations of 35%
"$0°$-twist", 15% "$15°$-twist", 40% "$33°$-twist", 5% "$60°$-twist" and 5% dis-
torted trans, with an uncertainty of perhaps ± 15%.

It is not easy to establish the precise shape of the distribution but
it may be concluded that the shape is distinctly non-Gaussian. If the
potential function for internal rotation had been a simple parabola
about ∅ = $0°$, the distribution would have been Gaussian with a root-mean-

square displacement from planarity of perhaps 10° to 20°.[5] The observed

flattening and broadening of the distribution can be attributed to the

nonbonded repulsion between the $Cl \cdot \cdot H_R$ atom pair which is strongest at

small values of ϕ.

E. Isopropyl Carboxaldehyde

A sample of isopropyl carboxaldehyde was obtained from Eastman

Organic Chemicals. Approximately twenty milliliters of the sample were

purified by fractional distillation. Gas chromatograms indicated that the

purity was not less than 99% pure.

The vapor from the liquid sample was introduced into the diffraction

chamber at a pressure of approximately 40 torr, the vapor pressure at

-7°C. An ice-water-NaCl bath was used to maintain this temperature.

Exposure times were approximately 4 seconds for the long camera distance

and 12 seconds for the middle camera distance. Data from four photographic

plates were analyzed for each camera distance using an IBM 7074 computer.

The $I_0(q)$ and $I_B(q)$ curves for the long and middle distances are illus-

trated in Figure 15.

The s-cis, s-trans and gauche configurations pictured in Figure 16

were tested in this structural analysis. In order to make the analysis

more manageable, it was again assumed that for each of these models all

C-C bonds had the same length and all C-H distances were equal.

Calculated and experimental f(r) curves were compared for different

---

[5]The potential energy of twist was assumed to have the form
$V_0(1 - \cos 2\theta)/2$ where V_0 is given the cyclopropyl carboxaldehyde value
of 2.5 to 10 kcal/mole.

Figure 15. A plot of the $I_o(q)$ and $I_B(q)$ curves for the long and middle camera distances of isopropyl carboxaldehyde

LONG CAMERA RANGE

C_3H_7CHO
EXP. INTENSITY

MIDDLE CAMERA RANGE

$I(q)$

$q\,(\text{Å}^{-1})$

54
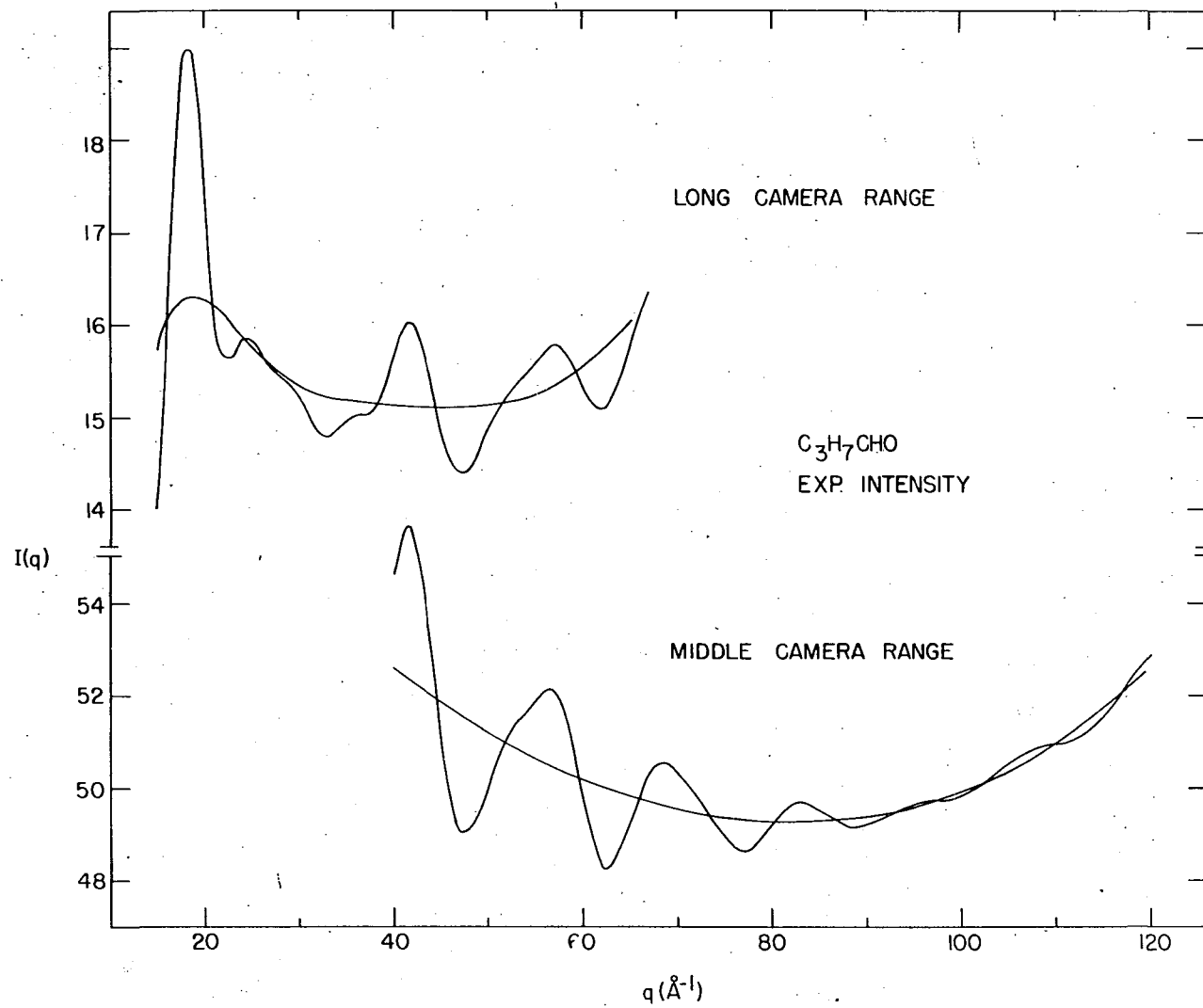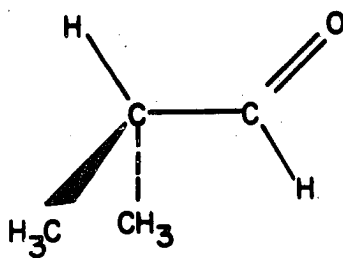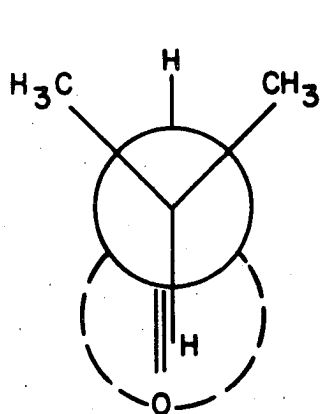
Figure 16. The s-cis, s-trans and gauche isomers of isopropyl carboxalde-
hyde

isomeric concentrations, assuming plausible values of the skeletal

parameters. Five of these sets of curves are shown in Figure 17. For
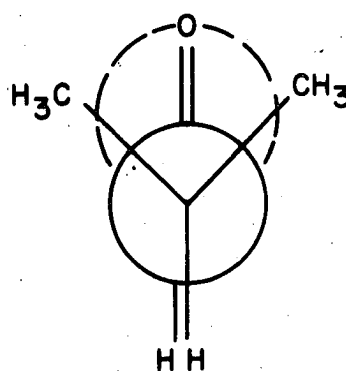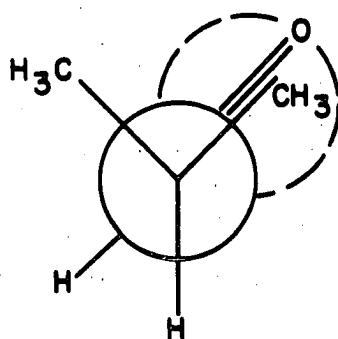
C_3H_7CHO, the relative strengths of the 2.8 and 3.5 Å nonbonded peaks are

a measure of the distribution among the rotational isomers. Using this

information, it can be easily seen in the plots mentioned above that the

concentration of s-cis isomer must be very small. It is also apparent

that the calculated f(r) curve for a pure gauche model compares quite well

with the experimental function. Consequently, the 2.8 and 3.5 Å peaks can

be ascribed to the two $O \cdot \cdot C_R$ nonbonded distances in this isomer.

Least squared fittings of experimental radial distribution curves

by calculated curves were run assuming various concentrations of s-cis,

s-trans and gauche isomers. The region from 2.5 to 4.2 Å was fitted, and

distances and amplitudes were optimized for each proportion. The best

fit, as implied by the lowest standard deviation, was obtained between

curves calculated from a concentration of 90% gauche and 10% s-trans

isomers. A plot of the complete experimental f(r) curve using this

model is shown in Figure 18. The values of parameters obtained from a

least squares analysis of this curve are listed in Table 7.

As in the analysis of cyclopropyl carboxaldehyde, an attempt was

made to obtain some information about the distribution in θ. The

potential energy for internal rotation of the carbonyl group was assumed

to have the form $V(\theta) = V_1(1 + \cos \theta)/2 + V_3(1 - \cos 3\theta)/2$. The energy

difference between the s-trans and gauche forms is approximately $3V_1/4$.

From the trans to gauche ratio, this energy difference was estimated and

the magnitude of V_1 was found to be approximately 1.1 kcal/mole. Least

squares fittings of the experimental f(r) curves by calculated curves were

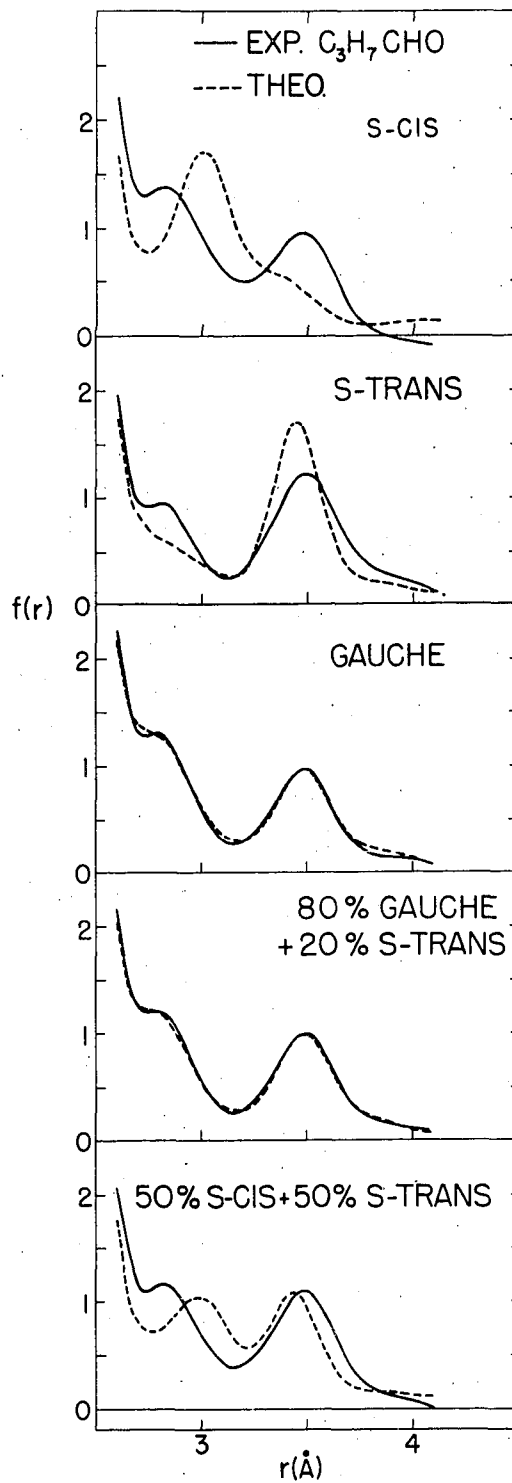Figure 17. Radial distribution curves for various concentrations of
isomers of isopropyl carboxaldehyde

Figure 18. A plot of the experimental radial distribution function for isopropyl carboxaldehyde
           with an assumed distribution of 90% gauche and 10% s-trans isomers. The lower curve
           is a plot of the difference between calculated and experimental radial distribution
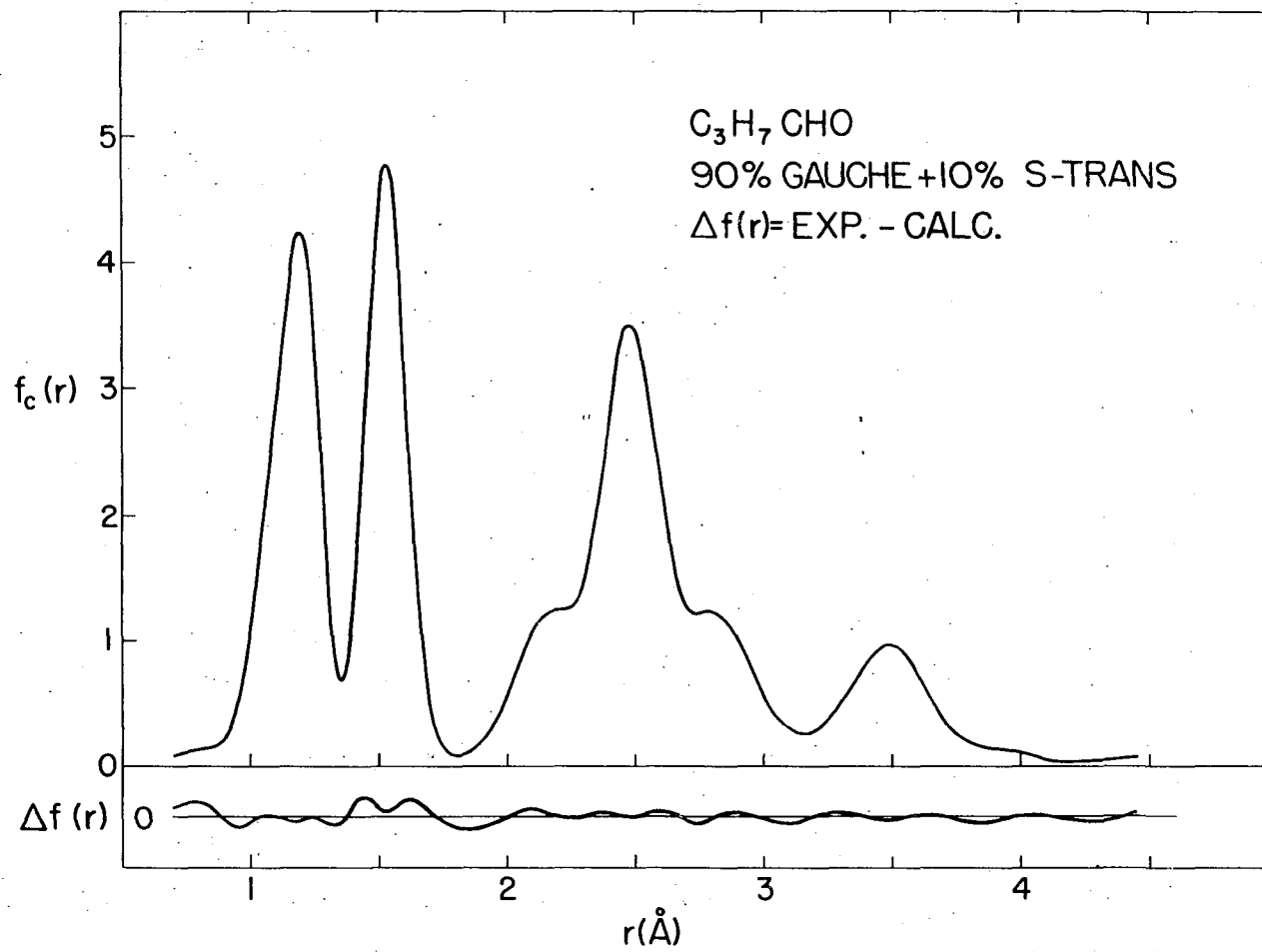   functions

Table 7. Molecular parameters for isopropyl carboxaldehyde derived from the radial distribution function (in Å units)

Distance	$r_g(0)$	$\sigma(r)$	l_g	$\sigma(l)$
C-H	1.127	0.012[a]	0.087	0.010[a]
C-C	1.528	0.002	0.044	0.002
C=O	1.206	0.008[a]	0.041	0.008[a]

$$\angle CCO = 123.3 \pm 1.7°, \quad \angle CCH_{aver} = 110.8 \pm 1.9°$$

$$\% \text{ gauche} = 90 \pm 15, \quad \% \underline{s}\text{-trans} = 10$$

[a]Because of severe overlapping of peaks in the $f(r)$ curve from which these parameters were obtained, the uncertainties have been arbitrarily taken as three times the standard devaitions calculated using the independent peak formula.

then run using various values of V_3 until optimum parameters were obtained. From the resulting standard deviations, it was found that the barrier to rotation, $V_3 + (V_1/2)$, is in excess of 2.5 kcal/mole.

F. N_2O_3-HF Complex

A liquid sample of a fractionally distilled 68°C constant boiling complex was received from Dr. F. Seel who proposed that the vapor was primarily NOF·6HF (8). Because of the extreme reactivity of the compound, the sample bulb, injection system and nozzle barrel used in taking the electron diffraction photographs were constructed entirely of Kel-F. The vapor from the liquid sample was injected into the diffraction chamber at room temperature and under a vapor pressure of approximately 85 torr. Exposure times were approximately 2.0 seconds for the long camera range

and 6.0 seconds for the middle camera range. Calculations involved in this analysis were done using the IBM 7074 computer. Long and middle distance intensity curves are shown in Figure 19.

The experimental radial distribution curve was first compared to the theoretical curve for a mixture of independent NOF and 6HF molecules. The absence of a peak in the $f(r)_{exp}$ curve near 1.52 Å, the reported NF distance in NOF (24), suggested that either there was no nitrosyl fluoride present or the NOF molecule was extremely distorted. Furthermore, the area associated with the theoretical NO peak was considerably less than that of the corresponding $f(r)_{exp}$ peak.

The unrefined radial distribution curve had three particularly prominent peaks: (a) one at approximately 0.94 Å which corresponds to the HF distance, (b) a second peak at $r = 1.19$ Å, a distance which is longer than the 1.13 Å NO distance in NOF, and (c) a smaller peak at approximately 2.20 Å.

The F··F and H··F nonbonded distances in polymeric hydrogen fluoride have been found to be approximately 2.55 ± 0.03 and 1.55 ± 0.06 Å, respectively (26). There is no peak in the 1.55 Å region of the experimental $f(r)$ curve and only a small peak in the 2.55 Å region. If more than two HF molecules are hydrogen-bonded to NOF, the magnitudes of the areas in the calculated curve which are associated with these nonbonded distances will exceed those in the $f(r)_{exp}$ curve. As a result, only the NOF·HF + 5HF and NOF·2HF + 4HF theoretical models were tested where first one, then two hydrogen fluorides were hydrogen-bonded to nitrosyl fluoride. The NOF segment itself was distorted to yield the best correspondence between experimental and calculated $f(r)$ curves. However, visual com-
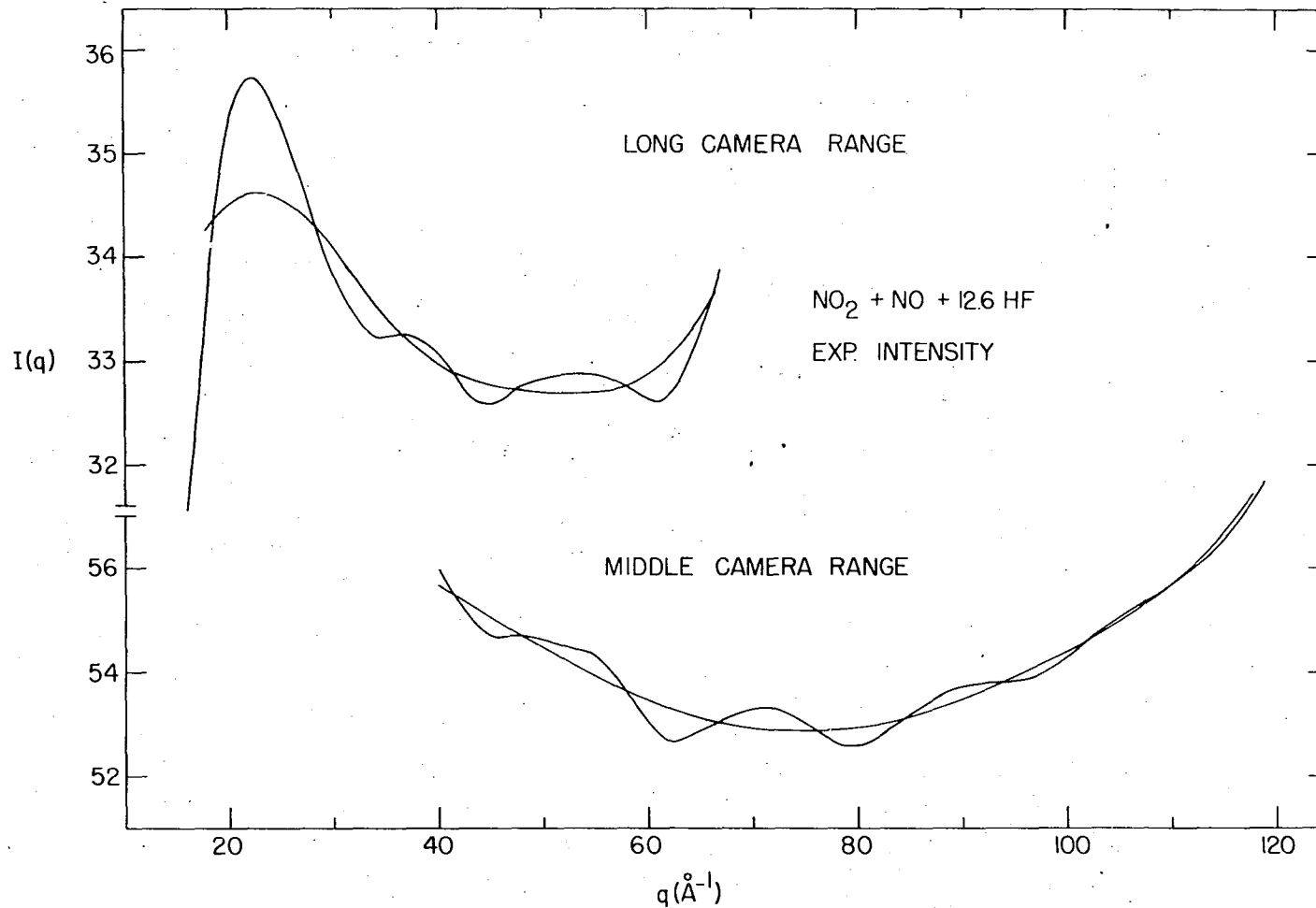
Figure 19. Experimental $I_0(q)$ and $I_B(q)$ curves for the long and middle camera distances of NO_2 + NO + 12.6 HF

parisons of these curves lend no support for the existence of the hydrogen-bonded structures.

Recent studies by R. S. Siegel[6] have shown that the 68°C boiling material is actually an azeotrope of composition N_2O_3 + 12.6 ± 0.2 HF. He demonstrated that this azeotrope is formed when water is added to a 95°C constant boiling complex or when NO is added to a NO_2-HF system. The 95°C material was called NOF·3HF by Seel, but Siegel showed that it is an azeotrope of N_2O_3, NOF and HF containing primarily NOF and HF molecules.

Seel reported that the 68°C material was prepared from NOCl and HF (8). His infrared analysis of the vapor from the sample gave a band which he described as being due to solvated NOF molecules. Siegel investigated spectra of 68°C boiling samples prepared from N_2O_3-HF and showed that the "NOF" band was probably due to NOCl formed by reaction of N_2O_3, HF and the AgCl windows of the cell. He also reported that the results of chemical analyses for nitrogen and fluorine performed on 68°C boiling samples prepared from both N_2O_3-HF and NOCl-HF mixtures were similar.

Dinitrogen trioxide is essentially completely dissociated to NO_2 and NO at room temperature and a pressure of approximately 80 torr (53). Figure 20 shows the radial distribution curve for NO_2 + NO + 12.6 HF. The peak at 2.20 Å corresponds to the O··O nonbonded distance in NO_2 while the shoulder at 2.55 Å may be associated with either the F··F nonbonded distance in HF polymer or the N··O distance in N_2O_4 (54) or

---

[6]Siegel, R. S., Brookhaven National Laboratory, Upton, New York, Products of the reaction between liquid nitrosyl chloride and hydrogen fluoride. Private communication. 1964.
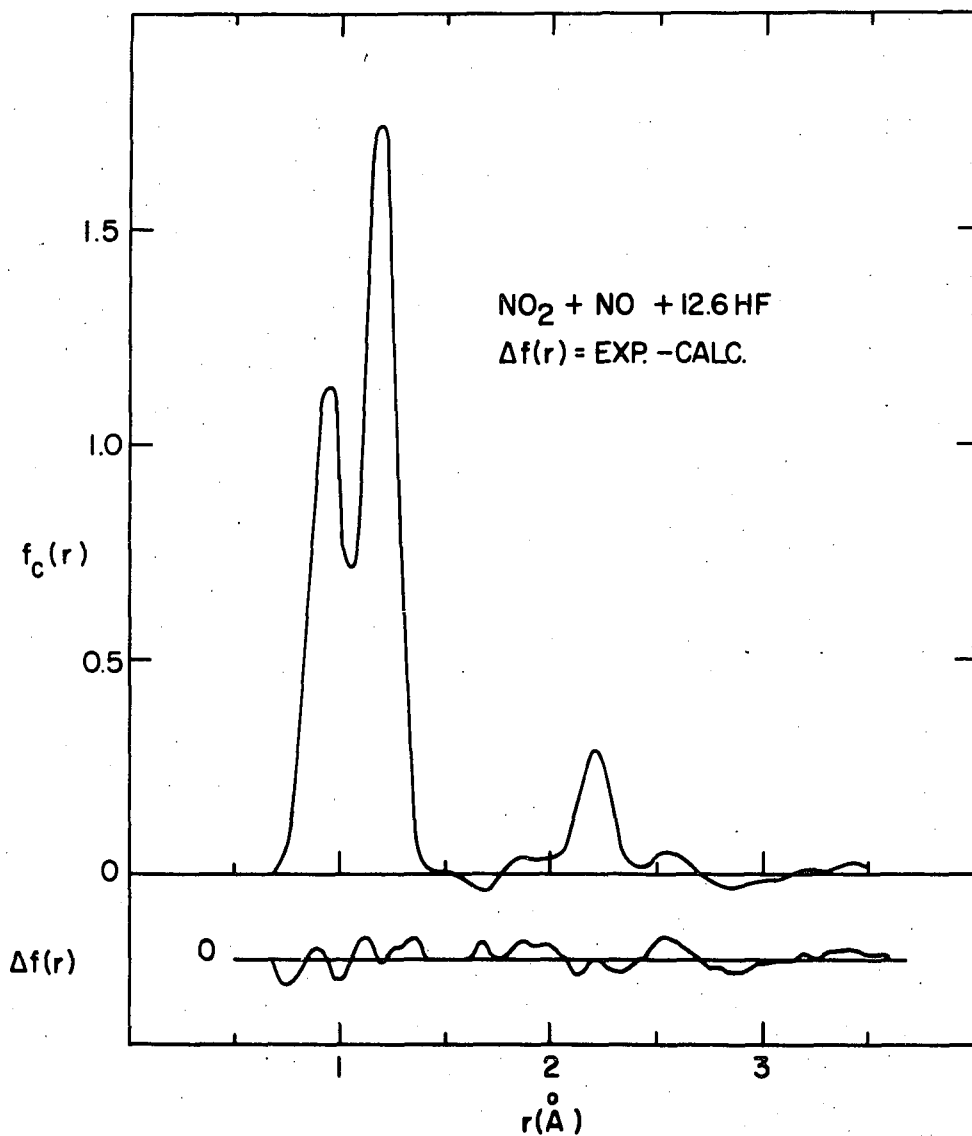
Figure 20. A plot of the experimental radial distribution curve for
NO_2 + NO + 12.6 HF. The lower curve is a plot of the
difference between the experimental and calculated radial
distribution functions

N_2O_3 (55). The concentrations of both of the last two molecules were probably less than 10% as suggested by the magnitude of the area of the 2.55 Å peak and the absence of a peak in the range from 1.6 to 1.7 Å, the NN distance in N_2O_4.

The shoulders at 1.85 and 2.55 Å could both be explained if NOCl impurities were present in the 68°C sample. A chloride analysis of the material, however, indicated that no such impurity was present.

The parameters determined for NO_2 + NO + 12.6 HF are listed in Table 8.

Table 8. Structural parameters for NO_2 + NO + 12.6 HF derived from the radial distribution function (in Å units)

Distance	$r_g(0)$	$\sigma(r)$	l_g	$\sigma(l)$
HF	0.944	0.004	0.069	0.003
NO	1.187	0.002	0.036	0.002
OO	2.204	0.012	0.061	0.012

G. Discussion of Structures

1. Ammonia and deuteroammonia

The center of gravity r_g obtained in the experiment is considered to be related to r_e, the equilibrium distance, by $r_g = r_e + \langle \Delta r \rangle$ where $\langle \Delta r \rangle$ is the instantaneous displacement of the bond length from r_e, averaged over the vibrational and rotational states. A rigorous calculation of the correction from mean to equilibrium distances, $\langle \Delta r \rangle$, was

carried out by Bartell et al. (5) for CH_4 and CD_4. They were thus able to make the first critical experimental comparison of the electron diffraction and spectroscopic methods, properly taking into account the different types of averaging over molecular motions.

Dr. K. Kuchitsu has carried out a normal-coordinate analysis of NH_3 and ND_3[7] using approximate values of cubic force constants evaluated from the spectroscopic data of Benedict and Plyler (11). He reported that $\langle \Delta r \rangle_{NH_3} = 0.018$ Å and $\langle \Delta r \rangle_{ND_3} = 0.015$ Å. These displacements were used in calculating mean NH and ND bond lengths from the spectroscopic r_e values. It was found, as shown in Table 9, that the calculated parameters are in good agreement with those derived from the present electron diffraction study.

2. Cyclopropyl carboxaldehyde

A comparison of results obtained from this study of cyclopropyl carboxaldehyde, cyclopropyl methyl ketone, cyclopropane carboxylic acid chloride and isopropyl carboxaldehyde with those from compounds containing similar bonds is made in Table 10. Bond distances and angles are in good agreement within the limits of experimental error.

The original object of this study of cyclopropyl carboxaldehyde was not so much to investigate its unknown conformational behavior as to determine the placement of the aldehyde carbon with respect to the ring. The investigation failed to detect any isomer approaching a nonclassical cyclopropyl carbinyl cation in configuration and provided no evidence

---

[7]Kuchitsu, K., Department of Chemistry, University of Tokyo, Bunkyo-Ku, Tokyo, Japan, Effect of anharmonic vibrations on the bond lengths of NH_3 and ND_3. Private communication. 1963.

Table 9. Comparison of results of structural determinations of NH_3 and ND_3 (in Å units)

Method		NH	ND	∠HNH	∠DND
IR[a]	r_o(exp)	1.0173	1.0155	107.78°	107.59°
	r_e	1.0124	1.0108	106.67°	106.70°
	r_g(calc)	1.0304	1.0258		
SMED[b]	r_g(exp)	1.0289 ±0.0019	1.0264 ±0.0017	106.03 ±1.32°	106.55 ±0.84°

[a]Infrared method. See reference 11. The order of magnitude of error in the distance parameters is approximately 0.001 Å as implied by the difference between r_e(NH) and r_e(ND).

[b]Present study using the sector-microphotometer method of electron diffraction.

for an unusually free $C_R \cdots C_0$ bond motion.

Nearly equal fractions of s-cis and s-trans molecules were present in the sample of C_3H_5CHO. Once recognized, this behavior is readily rationalized in terms of the π-electron character often proposed for the cyclopropane ring (56, 57, 58).

Extended Hückel calculations by Hoffmann (59) indicate that in the classical structure of the cyclopropyl carbinyl cation, the carbonium ion prefers to orient itself so that the $-CH_2^+$ and the tertiary hydrogen are coplanar. The results are in agreement with those of this electron diffraction study in conformational implications.

According to the π-electron viewpoint, cyclopropyl carboxaldehyde is analogous to 1,3-butadiene and acrolein, both of which have long been

Table 10. Comparison of results of various structural determinations (in $\overset{o}{A}$ units)

Molecule	CH^a	CC^a	CO^a	CCl^a	$\angle C\text{-}C\text{-}H$	$\angle C\text{-}C\text{-}O$	Method	Reference
C_3H_6	1.095 ±0.003	1.511 ±0.002			117.68 ±0.42°		$SMED^b$	18
CH_3CHO	1.086 ±0.005	1.5005 ±0.0050	1.2155 ±0.0020			123.92 ±0.1°	MW^c	21
C_3H_5CHO	1.115 +0.037 -0.021	1.507 ±0.002	1.216 +0.002 -0.018		117.1 ±3.1°	122.0 ±1.8°	SMED	present study
CH_3COCH_3	1.086 ±0.010	1.515 ±0.005	1.215 (assumed)		110.27 ±1.0°	121.88°	MW	60
$C_3H_5COCH_3$	1.126 ±0.015	1.510 ±0.003	1.225 ±0.011		117.2 ±2.8°	121.8 ±1.6°	SMED	present study
CH_3COCl	1.083 ±0.005	1.499 ±0.010	1.192 ±0.010	1.789 ±0.005	110.35 ±0.17°	127.08 ±0.17°	MW	61
C_3H_5COCl	1.107 ±0.021	1.506 ±0.002	1.197 ±0.009	1.797 ±0.009	120.7 ±3.9°	127.6 ±2.9°	SMED	present study
C_3H_7CHO	1.127 ±0.012	1.528 ±0.002	1.206 ±0.008		110.8 ±1.9°	123.3 ±1.7°	SMED	present study

[a] Parameters are r_o values for spectroscopic work and r_g values for electron diffraction results.

[b] Sector-microphotometer method of electron diffraction.

[c] Microwave method.

68

assumed to exist as planar and, presumably, s-cis and s-trans forms by virtue of conjugative stabilization. Firm evidence exists, however, only for the planar s-trans form of butadiene (62, 63). Similarly, microwave studies (64) reveal a number of torsional states of trans-acrolein but provide no evidence for the existence of cis despite estimations that a concentration of several percent would have been detectable.

The occurrence of nearly equal amounts of s-cis and s-trans isomers of cyclopropyl carboxaldehyde discloses a significant distinction between the cyclopropyl and vinyl groups. This distinction may be steric in origin. For example, clearances between the nonbonded atoms in cis-cyclopropyl carboxaldehyde are longer than in acrolein. A factor which mars this explanation, however, is that corresponding clearances in gauche-isopropyl carboxaldehyde, the predominant form in C_3H_7CHO, seem to be similar to those in cis-acrolein.

3. Cyclopropyl methyl ketone

The conformational behavior of cyclopropyl methyl ketone can be estimated from the behaviors of n-butane and cyclopropyl carboxaldehyde. The steric properties of the ketone are analogous to those of n-butane, and the nonsteric torsional potential should be similar to that of C_3H_5CHO. Nonbonded clearances in the antigauche and cis forms of $C_3H_5COCH_3$ resemble those in gauche and trans-butane, respectively (65, 66). Bonham and Bartell (65) have found that the trans form of n-butane is more stable than the gauche by approximately 600 cal/mole. If the energy difference between the cis and antigauche isomers of $C_3H_5COCH_3$ is assumed to have this value, then the approximate ratio between these

conformers can be estimated from the simplified equation

$$\exp(- \Delta E_{tot}/RT)_{ket} = (N_a/N_c)_{ket} = \exp(- \Delta E_{tors}/RT)_{ald}$$

$$x \exp(- \Delta E_{steric}/RT)_{but} \qquad . \qquad (24)$$

The fraction $(N_a/N_c)_{ket}$ represents the antigauche to cis ratio in

cyclopropyl methyl ketone, and $\exp(- \Delta E_{tors}/RT)_{ald}$ is evaluated from

the 55 : 45 cis-trans ratio in cyclopropyl carboxaldehyde. The term

$\exp(- \Delta E_{steric}/RT)_{but}$ is calculated using the trans-gauche energy differ-

ence in n-butane. Application of Equation 24 suggests that the equilibrium

concentration of $C_3H_5COCH_3$ should contain approximately 90% s-cis isomer.

This is in agreement with the results of the least squares f(r) analysis.

4. Cyclopropane carboxylic acid chloride

Replacing the adehydic hydrogen atom in C_3H_5CHO by a chlorine atom

substantially alters the conformational behavior of the cyclopropyl

carbonyl compound. It was found that approximately 95% of the total con-

centration of C_3H_5COCl consists of a broad distribution of isomers in the

region from about $\phi = + 30°$ to $- 30°$. The flat and broad shape of the

distribution is probably a result of the $Cl \cdot \cdot H_R$ nonbonded repulsion in

the "$0°$-twist" form.

5. Isopropyl carboxaldehyde

Isopropyl carboxaldehyde, unlike cyclopropyl carboxaldehyde, prefers

a given gauche configuration over the trans by a relative proportion of

approximately 4.5 : 1. The former may be considered a key fragment of

2-methylcyclohexanone, where the equatorial form comprises about 93% of

the total sample (67). <u>Gauche</u>-isopropyl carboxaldehyde is analogous to equatorial 2-methylcyclohexanone, and the trans form is analogous to the axial conformation except for its freedom from the $CH_3 \cdot \cdot H$ repulsions encountered in the axial derivative. The present results, unobscured by axial steric effects, show an intrinsic stabilization resulting from eclipsing the C=O and CH_3 groups. This is in agreement with the inferences made by Abraham and Pople (22), and Butcher and Wilson (23) with respect to the configuration of propionaldehyde.

6. N_2O_3-HF complex

The present electron diffraction study of the 68°C constant boiling material together with Siegel's report offer rather conclusive evidence that the complex is an azeotrope of N_2O_3 and HF. Bond lengths and angles determined in the present analysis are listed in Table 11. Also reported are HF and NO internuclear distances determined in other structural investigations. A 2 : 1 weighting of the reported NO distance in NO_2 with the NO bond length in NO gives an average length of 1.185 $\overset{o}{A}$ when $r(NO_2)$ is corrected to an r_g value. This is in good agreement with the least squares f(r) result of 1.187 $\pm$ 0.002 $\overset{o}{A}$.

Table 11. Comparison of results of various structural determinations of NO_2, NO and HF (in Å units)

Molecule	NO	HF	OO	Method	Reference
NO_2	1.197		2.206	MW[a]	32
NO	1.1552 ±0.0008			SMED[b]	33
$(NO_2 + NO)$	1.185[c]				
HF(polymer)		1.00 ±0.06		VED[d]	26
HF(monomer)		0.932		IR[e]	25
NO_2 + NO +12.6HF	1.187 ±0.002	0.944 ±0.004	2.204 ±0.012	SMED	present study

[a]Microwave r_o values.

[b]Sector-microphotometer method of electron diffraction. Distances are r_g parameters.

[c]Weighted average of NO distances in equimolar mixture of NO_2 and NO. Distances have been corrected to r_g values (68).

[d]Visual electron diffraction method.

[e]Infrared method. The reported r_e value has been corrected to r_g (69).

IV. SUMMARY

The structural parameters of ammonia and deuteroammonia were deter-
mined for comparison with the corresponding spectroscopic values. As
shown in Table 9, satisfactory agreement was obtained. Excellent
"internal" agreement between the results from the least squares f(r)
and least squares intensity methods was also achieved in this analysis.

It was hoped that an isotope effect on the bond length might be
observed in the NH_3-ND_3 system. The effect was not unequivocally
established in view of the uncertainty in the observed difference of
0.0025 ± 0.0021 Å.

The analysis of cyclopropyl carboxaldehyde yielded normal values
for bond angles and amplitudes of vibration and revealed no tendency of
the aldehyde to assume a nonclassical structure of the sort hypothesized
for its analog, the cyclopropyl carbinyl cation (70). It was found that
the vapor consisted of essentially an equal mixture of s-cis and s-trans
conformers. This behavior, which is surprisingly different from the
trans-gauche isomerization found in unstrained saturated aldehydes, was
rationalized in terms of the π-electron character of the cyclopropane
ring proposed by Walsh (58). The 2-fold barrier hindering rotation of
the aldehyde group was also estimated and found to be greater than 2.5
kcal/mole.

For cyclopropyl methyl ketone, an equilibrium concentration of 80%
s-cis isomer and 20% of an antigauche-distorted trans distribution was
found. The $H_M \cdots H_R$ nonbonded repulsions apparently destabilize the trans
configuration.

The equilibrium concentration of cyclopropane carboxylic acid chloride consists primarily of a broad distribution of "twist" isomers in the approximate range $-30° \leq \phi \leq +30°$. This distribution is distinctly non-Gaussian in shape. The $Cl\cdot\cdot H_R$ nonbonded repulsion in the "$0°$-twist" conformer destabilizes this planar isomer and is probably responsible for the broad and flat shape of the "twist" distribution.

The isomeric content of isopropyl carboxaldehyde, which may be considered to be a key fragment of 2-methylcyclohexanone, was found to be 90% gauche and 10% s-trans. Steric effects which had been proposed to account for the greater stability of equatorial 2-methylcyclohexanone over the axial form are not encountered in C_3H_7CHO. Hence, the presence of a large fraction of gauche isomer in the latter molecule implies a stabilization resulting from the eclipsing of a methyl group by a carbonyl group. The barrier to rotation of the aldehyde group was estimated to be in excess of 2.5 kcal/mole.

A 68°C constant boiling complex was studied by the electron diffraction technique. Although it was claimed by the supplier that the sample was NOF·6HF, this analysis, in conjunction with a study by Dr. R. S. Siegel, indicated that the vapor composition corresponded to NO_2 + NO + 12.6HF. The experimental NO, $O\cdot\cdot O$ and HF internuclear distances in the present sample are in good agreement with the values reported for independent determinations of NO_2, NO and HF molecules.

V. LITERATURE CITED

1. Bartell, L. S. and Brockway, L. O., Review of Scientific Instruments 25, 569 (1954).

2. Bastiansen, O., Hassel, O. and Risberg, E., Acta Chemica Scandinavica 9, 232 (1955).

3. Debye, P. P., Physikalische Zeitschrift 40, 66 (1939).

4. Karle, J. and Karle, I. L., Journal of Chemical Physics 18, 957 (1950).

5. Bartell, L. S., Kuchitsu, K. and deNeui, R. J., Journal of Chemical Physics 35, 1211 (1961).

6. Bartell, L. S., Kohl, D. A. and Carroll, B. L. Least squares determination of structures of gas molecules directly from electron diffraction intensities. Unpublished mimeographed paper. Ames, Iowa, Department of Chemistry, Iowa State University of Science and Technology. 1964.

7. Bonham, R. A. and Bartell, L. S., Journal of Chemical Physics 31, 702 (1959).

8. Seel, F., Birnkraut, W. and Werner, D., Chemische Berichte 95, 1264 (1962).

9. Dennison, D. M., Reviews of Modern Physics 12, 175 (1940).

10. Palik, E. D., Dissertation Abstracts 15, 2247 (1955).

11. Benedict, W. S. and Plyler, E. K., Canadian Journal of Physics 35, 1235 (1957).

12. Weiss, M. and Strandberg, M. W. P., Physical Review 83, 567 (1951).

13. Cummings, C. and Welsh, H. L., Journal of Chemical Physics 21, 1119 (1953).

14. Almenningen, A. and Bastiansen, O., Acta Chemica Scandinavica 9, 815 (1955).

15. Pauling, L. and Brockway, L. O., Journal of the American Chemical Society 59, 1223 (1937).

16. Bastiansen, O. and Hassel, O., Tidsskrift for Kjemi, Bergvesen og Metallurgi 6, 71 (1946). Original available but not translated; abstracted in Chemical Abstracts 40: 6059. 1946.

17. Sinha, S. P., Journal of Chemical Physics 18, 217 (1950).

18. Bastiansen, O., Fritsch, F. N. and Hedberg, K., Acta Crystallographica 17, 538 (1964).

19. Ackermann, P. G. and Mayer, J. E., Journal of Chemical Physics 4, 377 (1936).

20. Stevenson, D. P., Burnham, H. D. and Schomaker, V., Journal of the American Chemical Society 61, 2922 (1939).

21. Kilb, R. W., Lin, C. C. and Wilson, E. B., Journal of Chemical Physics 26, 1695 (1957).

22. Abraham, R. J. and Pople, J. A., Molecular Physics 3, 609 (1960).

23. Butcher, S. S. and Wilson, E. B., Journal of Chemical Physics 40, 1671 (1964).

24. Magnuson, D. W., Journal of Chemical Physics 19, 1071 (1951).

25. Naude, S. M. and Verleger, H., Proceedings of the Physical Society (London), Section A, 63, 470 (1950).

26. Bauer, S. H., Beach, J. Y. and Simons, J. H., Journal of the American Chemical Society 61, 19 (1939).

27. Smith, D. F., Journal of Chemical Physics 28, 1040 (1958).

28. Franck, E. U. and Meyer, F., Zeitschrift für Elektrochemie 63, 571 (1959).

29. Briegleb, V. G. and Strohmeier, W., Zeitschrift für Elektrochemie 57, 668 (1953).

30. Maclean, J. N., Rossotti, F. J. C. and Rossotti, H. S., Journal of Inorganic Nuclear Chemistry 24, 1549 (1962).

31. Moore, G. E., Journal of the Optical Society of America 43, 1045 (1953).

32. Bird, G. R., Journal of Chemical Physics 25, 1040 (1956).

33. Bartell, L. S. and Kuchitsu, K., Journal of the Physical Society of Japan 17, 20 (1962).

34. Nichols, N. L., Hause, C. D. and Noble, R. H., Journal of Chemical Physics 23, 57 (1955).

35. Hauptman, H. and Karle, J., Physical Review 77, 491 (1950).

36. Atoji, M., Acta Crystallographica $\underline{10}$, 291 (1956).

37. Bewilogua, L., Physikalische Zeitschrift $\underline{32}$, 740 (1931).

38. Debye, P. J. W., Mathematics and Physics $\underline{4}$, 133 (1925).

39. Kuchitsu, K. and Bartell, L. S., Journal of Chemical Physics $\underline{35}$, 1945 (1961).

40. Bonham, R. A. and Ukaji, T., Journal of Chemical Physics $\underline{36}$, 72 (1962).

41. Bartell, L. S., Brockway, L. O. and Schwendeman, R. H., Journal of Chemical Physics $\underline{23}$, 1854 (1955).

42. Bartell, L. S. and Brockway, L. O., Journal of Chemical Physics $\underline{32}$, 512 (1960).

43. Bartell, L. S., Journal of Applied Physics $\underline{31}$, 252 (1960).

44. Bonham, R. A. An electron diffraction investigation of free hydrocarbon molecules. Unpublished Ph.D. thesis. Ames, Iowa, Library, Iowa State University of Science and Technology. 1958.

45. Bastiansen, O., Hedberg, L. and Hedberg, K., Journal of Chemical Physics $\underline{27}$, 1311 (1957).

46. Morino, Y., Kuchitsu, K. and Murata, Y., Acta Crystallographica $\underline{16}$, A129 (1963).

47. Ransil, B. J., Reviews of Modern Physics $\underline{32}$, 245 (1960).

48. Bersohn, R., Journal of Chemical Physics $\underline{32}$, 85 (1960).

49. Bader, R. F. W. and Jones, G. A., Journal of Chemical Physics $\underline{38}$, 2791 (1963).

50. Scarborough, J. B. Numerical mathematical analysis. 2nd ed. Baltimore, Maryland, The John Hopkins Press. 1950.

51. Bartell, L. S. and Carroll, B. L. Electron diffraction study of diborane and deuterodiborane. Unpublished mimeographed paper. Ames, Iowa, Department of Chemistry, Iowa State University of Science and Technology. 1964.

52. Pauling, L. Nature of the chemical bond. 3rd ed. Ithaca, New York, Cornell University Press. 1960.

53. Beattie, I. R. and Vosper, A. J., Journal of the Chemical Society $\underline{1961}$, 2106.

54. Broadley, J. S. and Robertson, J. M., Nature 164, 915 (1949).

55. Devlin, J. P. and Hisatsune, I. C., Spectrochimica Acta 17, 218 (1961).

56. Cromwell, N. H. and Hudson, G. V., Journal of the American Chemical Society 75, 872 (1953).

57. Kosower, E. M., Proceedings of the Chemical Society 1962, 25.

58. Walsh, A. D., Transactions of the Faraday Society 45, 179 (1949).

59. Hoffmann, R., Journal of Chemical Physics 40, 2480 (1964).

60. Swalen, J. D. and Costain, C. C., Journal of Chemical Physics 31, 1562 (1959).

61. Sinnott, K. M., Journal of Chemical Physics 34, 851 (1961).

62. Almenningen, A., Bastiansen, O. and Traetteberg, M., Acta Chemica Scandinavica 12, 1221 (1958).

63. Marais, D. J., Sheppard, N. and Stoicheff, B. P., Tetrahedron 17, 163 (1962).

64. Wagner, R., Fine, J., Simmons, J. W. and Goldstein, J. H., Journal of Chemical Physics 26, 634 (1957).

65. Bonham, R. A. and Bartell, L. S., Journal of the American Chemical Society 81, 3491 (1959).

66. Bartell, L. S. and Kohl, D. A., Journal of Chemical Physics 39, 3097 (1963).

67. Allinger, N. L. and Blatter, H. M., Journal of the American Chemical Society 83, 994 (1961).

68. Laurie, V. W. and Herschbach, D. R., Journal of Chemical Physics 37, 1687 (1962).

69. Bartell, L. S., Journal of Chemical Physics 23, 1219 (1955).

70. Mazur, R. H., White, W. H., Semenow, D. A., Lee, C. C., Silver, M. C. and Roberts, J. D., Journal of the American Chemical Society 81, 4390 (1959).

VI. ACKNOWLEDGMENTS

I wish to thank Dr. L. S. Bartell for the valuable advice and assistance given during the course of this research.

I would also like to thank Dr. K. Kuchitsu for taking the diffraction pictures of ammonia and deuteroammonia and Dr. H. B. Thompson for his many helpful suggestions.

For their aid and advice, I wish to express my gratitude to Ben Carroll and Harlan Higginbotham.

I also want to thank Miss M. Dunlap and Miss A. Parks for their help in the analyses of cyclopropyl carboxaldehyde and cyclopropane carboxylic acid chloride.

And finally I wish to thank my wife, to whom I dedicate this work, for the patience and understanding she has shown and the moral support she has given throughout this study.